

For Reference

NOT TO BE TAKEN FROM THIS ROOM

Ex LIBRIS
UNIVERSITATIS
ALBERTAENSIS





Digitized by the Internet Archive
in 2020 with funding from
University of Alberta Libraries

<https://archive.org/details/Berntsen1971>

THE UNIVERSITY OF ALBERTA
COMPARATIVE HEAT FLUX MEASUREMENTS IN THE
SURFACE BOUNDARY LAYER

by



LLOYD BERNTSEN

A THESIS
SUBMITTED TO THE FACULTY OF GRADUATE STUDIES
IN PARTIAL FULFILMENT OF THE REQUIREMENTS FOR THE DEGREE
OF MASTER OF SCIENCE

DEPARTMENT OF GEOGRAPHY

EDMONTON, ALBERTA

FALL, 1971

THE UNIVERSITY OF ALBERTA
FACULTY OF GRADUATE STUDIES

The undersigned certify that they have read, and recommend to the Faculty of Graduate Studies for acceptance, a thesis entitled, "COMPARATIVE HEAT FLUX MEASUREMENTS IN THE SURFACE BOUNDARY LAYER", submitted by LLOYD BERNTSEN in partial fulfilment of the requirements for the degree of Master of Science.

ABSTRACT

The objective of this study was to compare heat flux measurements in the surface boundary layer, using a fluxatron and a sonic anemometer-thermometer. These two instruments measure, independently, the fluctuations in temperature and vertical wind. The heat fluxes are obtained from these data using the eddy correlation technique. All measurements were carried out under unstable conditions. Comparative variance and covariance spectra are presented and comparisons are made with the $-5/3$ power law and with the results obtained by other authors.

Both of the instrument systems were being subjected to an initial evaluation at the University of Alberta. Numerous calibration problems were encountered, some of which have not yet been solved. In particular, the non-linear response at low wind speeds of the fluxatron's propeller anemometer remains as the most difficult problem.

Apart from the calibrations, the two instruments appear to measure the fluctuating quantities with quite close agreement. This result is based on normalized spectra and cospectra which are independent of calibration errors, since in each case the normalizing factor contains the same calibrations as the spectral estimates.

The final analysis of comparative heat fluxes yields results from the sonic anemometer-thermometer data which are approximately twice as large as those from the fluxatron data. This large difference is attributed to the calibration problems mentioned.

ACKNOWLEDGEMENTS

I am sincerely grateful for the assistance and advice of many people in the realization of this thesis.

First, I would like to thank my thesis supervisor, Dr. K. D. Hage, for his many helpful suggestions during the course of this study. Thanks are also due to Professor R. W. Longley and Dr. E. R. Reinelt for advice during the final stages of the project.

I would also like to thank Mr. F. R. McDougall and Mr. J. D. Steenbergen for considerable assistance in the preparation of the instruments and in the data collection. Also, I am grateful to Mr. N. W. Ouelette of the Geophysics Division, Department of Physics for assistance in the analog to digital conversion and in the programming of the "fast Fourier transform".

I would like to thank the Canadian Meteorological Service for supporting me while on educational leave.

Finally, I would like to thank Mrs. L. Smith for typing the initial and final drafts.

TABLE OF CONTENTS

	PAGE
ABSTRACT	iii
ACKNOWLEDGEMENTS	iv
TABLE OF CONTENTS	v
LIST OF TABLES	vi
LIST OF FIGURES	vii
Chapter	
I. INTRODUCTION	1
Basic Theory	1
History of Flux Measurements	3
II. EXPERIMENTAL SETUP	6
Site	6
Instrument Setup	7
Sonic Anemometer-Thermometer	7
Fluxatron	12
III. DATA COLLECTION AND REDUCTION	17
Data Collection	17
Analog to Digital Conversion	20
IV. SPECTRAL ANALYSIS	23
V. DISCUSSION OF RESULTS	25
Coherences	25
Wind Spectra	31
Temperature Spectra	40
Cospectra Between Wind and Temperature	45
Comparative Heat Fluxes	51
VI. SUMMARY	56
BIBLIOGRAPHY	58

LIST OF TABLES

TABLE		PAGE
1.	Timetable of observational samples	19
2.	Temperature at 115m and 17m on the CN Tower in Edmonton	19
3.	Summed variances of vertical wind	36
4.	Summed variances of temperature	36
5.	Heat fluxes from integration of cospectra	55
6.	Heat fluxes from covariances of digitized data . . .	55

LIST OF FIGURES

FIGURE		PAGE
1.	Air photograph of the University of Alberta farm at Ellerslie, showing the location of the meteorological site in relation to the farm buildings and trees	8
2.	Photograph of the individual masts and sensor arrays of the fluxatron and the sonic anemometer-thermometer (S.A.T.)	9
3a.	Close-up photograph of the two sensor arrays	13
3b.	Photograph of fluxatron console, S.A.T. console, and chart recorders	13
4.	Comparative chart recorder traces of fluxatron vertical wind and S.A.T. vertical wind	14
5.	Coherence between S.A.T. wind and fluxatron wind over the low frequency range of analysis	27
6.	Coherence between S.A.T. wind and fluxatron wind over the high frequency range of analysis	28
7.	Coherence between S.A.T. temperature and fluxatron temperature over the low frequency range of analysis	29
8.	Coherence between S.A.T. temperature and fluxatron temperature over the high frequency range of analysis	30
9.	Absolute variance spectra of vertical wind over the low frequency range of analysis, with the ordinate calibrated in cm^2/sec^2 . For Figures 9 to 16, the square plot symbols represent analyses of the S.A.T. data, and the round plot symbols represent analyses of the fluxatron data	32
10.	Absolute variance spectra of vertical wind over the high frequency range of analysis	35

FIGURE		PAGE
11.	Normalized variance spectra of vertical wind over the low frequency range of analysis	38
12.	Normalized variance spectra of vertical wind over the high frequency range of analysis	39
13.	Absolute variance spectra of temperature over the low frequency range of analysis, with the ordinate calibrated in $(^{\circ}\text{C})^2$	41
14.	Absolute variance spectra of temperature over the high frequency range of analysis	42
15.	Normalized variance spectra of temperature over the low frequency range of analysis	43
16.	Normalized variance spectra of temperature over the high frequency range of analysis	44
17 to 20.	Absolute cospectra between vertical wind and temperature over the low frequency range of analysis, with the ordinates calibrated in milliwatts/cm ² . The square plot symbols for Figures 17 to 22 represent analyses of the fluxatron data, and the round plot symbols represent analyses of the S.A.T. data	47
21 and 22.	Normalized cospectra between wind and temperature over the low frequency range of analysis	52

CHAPTER I

INTRODUCTION

During the past twenty years numerous instruments have been developed in attempts to measure turbulent fluxes in the surface boundary layer. A problem common to all measurements is that there is no direct calibration available. Hence, to gain confidence in any of the instruments, comparative but independent measurements must be made of the same turbulent quantity. The object of this research was to make comparative measurements of turbulent heat flux using a fluxatron and a sonic anemometer-thermometer. The comparisons were made primarily in the frequency domain by calculating the power spectra of the two winds and the two temperatures, followed by computation of cospectra of wind and temperature for each instrument.

Basic Theory

Turbulent heat flux can be measured by instruments which utilize the eddy correlation technique. Considering an element of air of density ρ , vertical velocity w , and temperature T , passing a fixed point, the instantaneous heat flux at that point is $C_p \rho w T$, where C_p is the specific heat at constant pressure. The average heat flux is then $C_p \overline{\rho w T}$ where the bar denotes a time average at a fixed point. Expressing each of the variables ρ , w , and T as a mean quantity plus a fluctuation about that mean the expression for the heat flux becomes

$$H = C_p [(\bar{\rho} + \rho') (\bar{w} + w') (\bar{T} + T')] .$$

If there is no significant convergence or divergence beneath the point of observation it can be assumed that $\bar{\rho}w$ will be very small. The heat flux expression can then be expanded to give

$$H = C_p [\bar{\rho} \overline{w'T'} + \bar{w} \overline{\rho'T'} + \overline{\rho'w'T'}] .$$

The second term in the bracket is neglected since the mean vertical wind is assumed to be nearly zero. The third term is also assumed to be small compared to the first, but this is not quite so obvious. Businger and Miyake (1968) measured the magnitude of the third term, as compared to the first, using a sonic anemometer-thermometer and found a ratio of 0.0014, and concluded that this term is indeed negligible. Thus, the final expression for the turbulent heat flux can be written

$$H = C_p \bar{\rho} \overline{w'T'} .$$

To use this relationship, simultaneous readings of vertical wind and temperature are required at the same point in space. Also, the instrument must measure all the fluctuations which contribute to the flux. Therefore, it must have sensor response such that it can measure the entire frequency range contributing to the flux.

In the frequency domain the turbulent heat flux can be written

$$H = C_p \bar{\rho} \int_0^{\infty} \phi_{wT}(n) dn$$

where $\phi_{wT}(n)$ is the cospectrum between vertical wind and temperature, and where n is frequency. In practice, the limits of the integrand are determined by sensor response and sample lengths. Businger et al (1967) suggest that the lower and upper frequency limits required to contain

95 per cent of the covariance can be approximated by $10^{-3} \bar{u}/Z$ and $5 \bar{u}/Z$ respectively, where \bar{u} is the mean wind speed at the height Z of the observations.

History of Flux Measurements

Swinbank (1951) was the first to take simultaneous measurements of w and T and to correlate them. His sensors were hot-wire anemometers and thermocouples. In general, his computed values of H were too small, caused primarily by too short an averaging time. The short averaging time was necessary in order to limit the number of manual computations during analysis.

This problem led to the development of an instrument which could measure fluctuating quantities simultaneously and perform the multiplications and integrations automatically (Dyer, 1961).

The basic instrument went through numerous development stages as described by Dyer and Mayer (1965), and Dyer, Hicks and King (1967), to the current version, called the fluxatron (Hicks, 1970). This instrument uses as sensors a propeller anemometer to measure w and a bead thermistor to measure T .

Throughout the period during which the fluxatron was developed, considerable developmental work was being done on an instrument which computed w and T fluctuations by measuring the transit times of sound waves (Kaimal and Businger, 1963, 1963a). This instrument was developed from earlier instruments which measured the fluctuations of wind or temperature, but not both. Barret and Suomi (1949) reported on an early attempt to develop a pulse-type sonic thermometer. Davidson and Lettau (1953) used a sonic anemometer to measure fluctuations in vertical wind. Schotland (1955) used a sonic anemometer to measure

horizontal wind. Considerable work in this field was also being done in both the USSR and Japan at that time. Gurvich (1959) described an acoustic microanemometer developed for use in turbulence studies. Mitsuta (1966) described a sonic anemometer-thermometer which had been developed in Japan.

In practice, the wind and temperature fluctuations are obtained with a sonic instrument by measuring the difference and sum of transit times for signals of two different frequencies travelling in opposite directions along a well defined path. The main advantages of such an instrument are, first, that the simultaneous observations of w and T are taken over the same path, and second, that the response times of the sensors are very short. The instrument developed using this technique is called a sonic anemometer-thermometer, commonly abbreviated S.A.T.

Since both of these instruments to measure the heat flux have been developed without an absolute calibration, the only way to gain confidence in the method is to make extensive comparisons between the two independent flux measuring instruments. Such a comparison experiment has been described by Businger et al (1967), in which they compared a S.A.T. with a fluxatron and an evapotron. They reported agreement only within a factor of two, with the fluxatron observations giving higher heat fluxes than those of the S.A.T. This disagreement of results was in the opposite direction from what might have been expected in view of the response times of the two instruments. Their instruments were mounted on masts 5 m apart and they suggested that this may be too much separation, particularly if, as they postulated, the convective elements consist of horizontal rolls with their length

axis in the direction of the mean wind.

A more recent instrument comparison test was made by Businger et al (1969). This test involved comparisons between two independently developed S.A.T.'s. One was a continuous wave S.A.T. developed at the University of Washington, and the other a pulse-type S.A.T. developed at Kyoto University in Japan. In computing comparative spectra of w and T , as well as cospectra between w and T , they found general agreement to within ± 15 per cent, which tends to give confidence in the performance of a S.A.T.

A further study, performed by Wesely, Thurtell and Tanner (1969), compared heat flux measurements made with six independent sets of instruments. These instruments included a one-dimensional S.A.T., a three-dimensional S.A.T., an evapotron (Dyer and Mayer, 1965), a pressure-sphere anemometer, an energy-balance calculation, and an aerodynamic calculation based on wind and temperature profiles. All of their results were presented in graphical form only, and were based on analyses in the time domain. The sets of results appeared to be in good agreement with each other, although the evapotron results showed quite wide fluctuations. These fluctuations are interpreted as being due to a time constant of only one minute used in averaging the wind and temperature data.

The object of the research for this thesis was to compare recent versions of the fluxatron and S.A.T. and to compute comparative variance spectra of heat flux using these two instruments.

CHAPTER II

EXPERIMENTAL SETUP

Site

The experiments were carried out during the summer of 1970 on the University of Alberta farm at Ellerslie, three and one-half miles south of the city limits of Edmonton. It is located at $53^{\circ}24'N$, $113^{\circ}33'W$, and is at an elevation of 2276 ft above mean sea level.

The area is not an ideal micrometeorological site, but was chosen because of the availability of other meteorological data such as wind and temperature observations, and the access to 60-cycle power. The surrounding land is quite flat to the north, west and south of the site and has a downward slope of approximately one in fifty to the east. The surface cover in the vicinity of the site is mown grass with wooded areas 400 m to the west of the site and 200 m to the southeast. A group of farm buildings is located approximately 140 m north (see Figure 1), and a second group of buildings 400 m south of the site. The meteorological site is equipped with two masts, Stevenson screen, evaporation pan and other recording instruments, and during the experiments the fluxatron and S.A.T. were set up to the windward of these fixed instruments. During the runs used for analysis in this experiment the wind direction varied from west to northwest, so that the trees to the west were the main cause of inhomogeneity of terrain in the windward direction.

Instrument Setup

The two recording instruments, a fluxatron and a S.A.T., were set up on individual, portable masts with the mid-point of the array of sensors at 3.5 m above the ground. They were set up in a configuration such that the S.A.T. and fluxatron sensors were 0.5 m apart, across the direction of and facing into the wind (see Figure 2).

Sonic Anemometer-Thermometer

The development and successful application of the continuous-wave sonic technique for the measurement of vertical velocity and temperature has been pioneered by Kaimal and Businger (1963, 1963a). The instrument used in the present experiment is very similar to their original design. Two sonic signals of different frequencies are transmitted in opposite directions along two acoustic paths which are side by side and 7.6 cm apart. Different frequencies are employed so that filters can be used to reduce interference between the two channels. The phase of each received signal is compared to that of a reference signal, and the wind and temperature are then obtained by means of appropriate analog circuitry.

Kaimal and Businger (1963) have described the theory of the S.A.T. Briefly, this is as follows. If t_1 is the transit time for a sonic wave front travelling along one of the acoustic paths, and t_2 the transit time for a wave front travelling along the opposite path, then the fluctuations in transit times t'_1 and t'_2 are given by

$$t'_2 - t'_1 = \frac{2dw'}{\bar{c}^2} \quad (1)$$

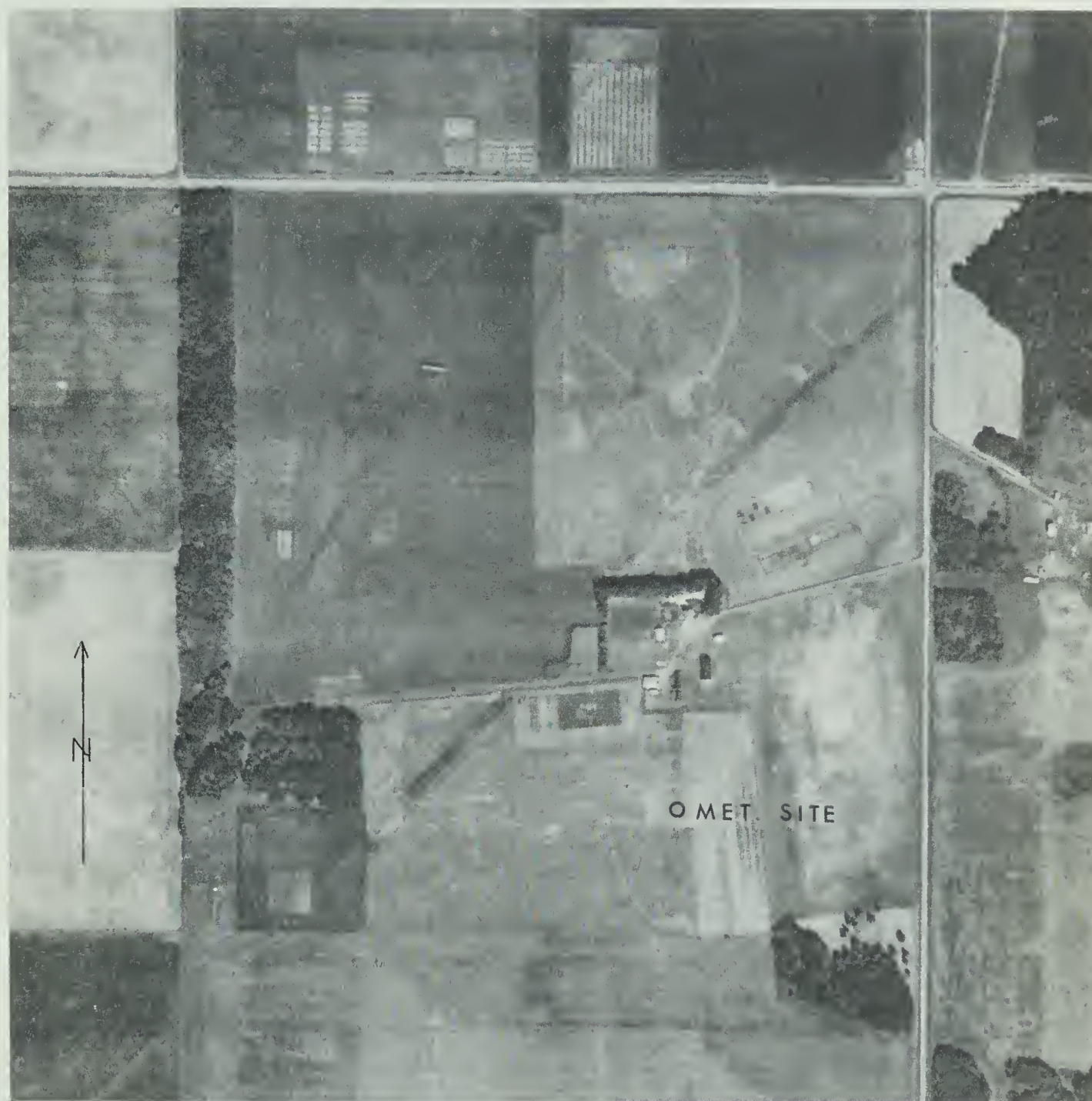


FIGURE 1

Air photograph of the University of Alberta farm at Ellerslie, showing the location of the meteorological site in relation to the farm buildings and trees.

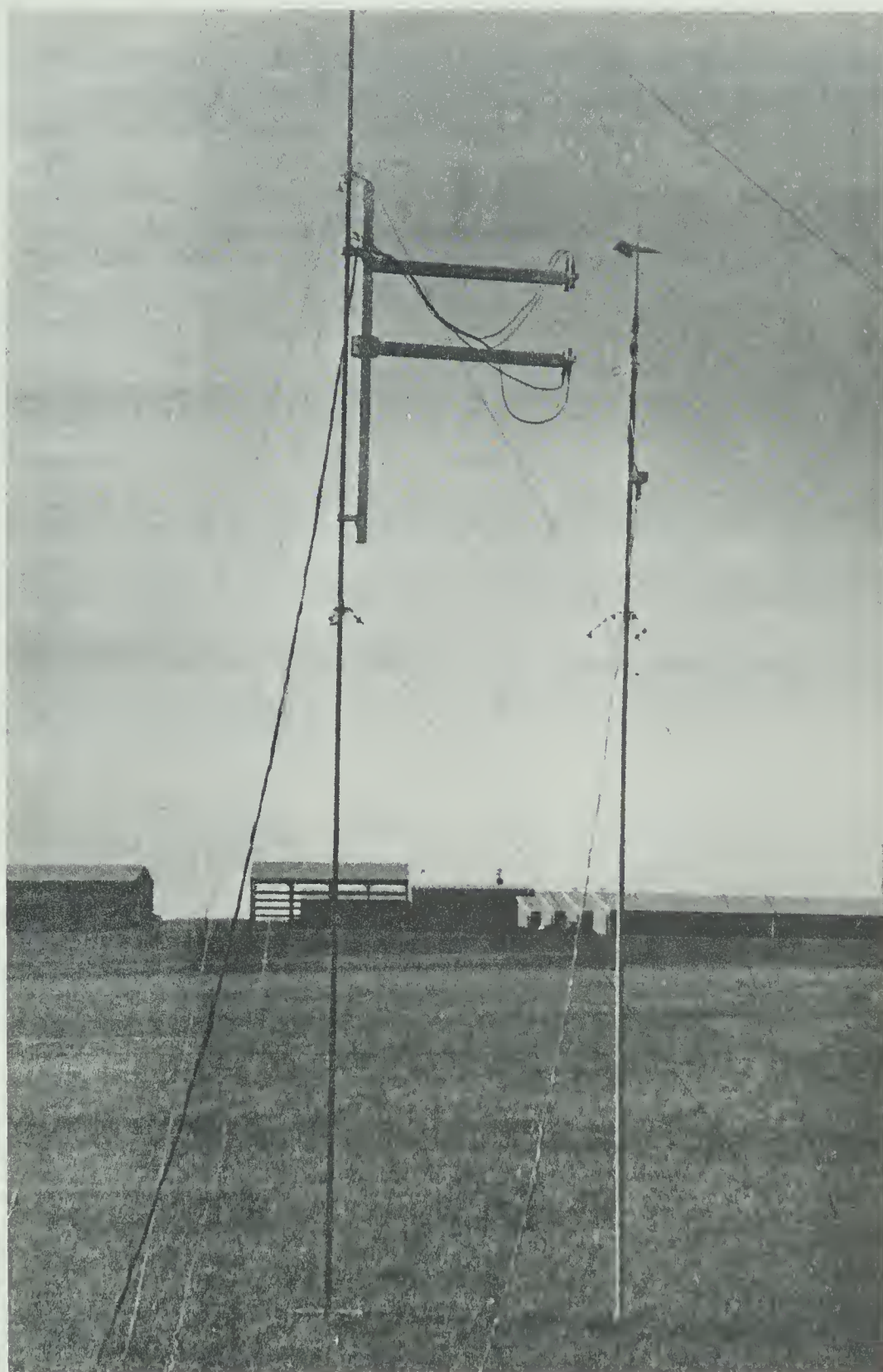


FIGURE 2

Photograph of the individual masts and sensor arrays of the fluxatron and the sonic anemometer-thermometer (S.A.T.).

$$t_2' + t_1' = \frac{-2d}{\bar{C}} \left[\frac{T'}{2\bar{T}} + \frac{0.16e'}{p} - \frac{\bar{u}u'}{\bar{C}^2} \right] \quad (2)$$

where d is the acoustic path length, w the vertical wind component, u the horizontal wind component, C the speed of sound in calm air, T the absolute temperature, e the vapour pressure of water, and p the atmospheric pressure. The bars denote time averages and the primes are fluctuations about these averages.

The difference $(t_2' - t_1')$ is dependent on w' only, while $(t_2' + t_1')$ depends on T' , e' and u' . Normally, for measurement over dry land, the term $0.16e'/p$ is very small, and also $\left| \frac{\bar{u}u'}{\bar{C}^2} \right| \ll \left| \frac{T'}{2\bar{T}} \right|$, except for cases of strong, gusty winds when both \bar{u} and u' are relatively large.

The fluctuations in transit time can be expressed in terms of phase fluctuations by putting

$$t_1' = \frac{-\phi_1'}{2\pi f_1} \quad \text{and} \quad t_2' = \frac{-\phi_2'}{2\pi f_2}.$$

Then, assuming light winds and dry air, the results become

$$\phi_2' - K\phi_1' = \frac{2\pi K f_1 d w'}{\bar{C}^2} \quad (3)$$

$$\phi_2' + K\phi_1' = \frac{2\pi K f_1 d T'}{\bar{C} \bar{T}} \quad (4)$$

where $K = f_2/f_1$, the ratio of the two frequencies used. To prevent interference between the two channels, identical as well as harmonic frequencies should be avoided. In this experiment the frequencies used are 7.5 kHz and 5.0 kHz as f_1 and f_2 respectively. The choice of d is such that it is small enough to measure the high frequency eddies, yet

large enough so that turbulence generated by the transducers does not affect the operation of the instrument. In this experiment d was set at 26.0 cm.

To use this instrument for the measurement of vertical wind and temperature fluctuations, it is necessary to calibrate the output signals. This is done by setting $\phi'_1 = 0$ and $\phi'_2 = 30$ degrees in (3) and (4) and measuring the output voltage, and similarly setting $\phi'_1 = 0$ and $\phi'_2 = -30$ degrees and again measuring the output. This procedure gives calibrations for w' and T' and should be repeated about once an hour, particularly if the mean temperature \bar{T} is changing significantly.

The limitations in accuracy of this instrument arise from three main sources of error. The first of these is the approximations made in the theoretical development. Over dry land the humidity term is negligible. However, over wet land, or over water, appropriate corrections would have to be made in the temperature calibration. The error caused by neglecting the horizontal velocity term is very small for light winds, but becomes significant for winds greater than 5 m/sec when u' is large.

A second source of possible error is random noises and reflections. High frequency noises may cause interferences, although these can usually be controlled at a meteorological site. The reflections of the transmitted signals from large, flat surfaces could cause interference, but if the only such surface is the earth, Kaimal and Businger (1963) have shown that the reflected wave is insignificant above heights of 2 m.

The third possible type of error is that caused by the operator. One of these is in the measurement of such quantities as d and \bar{T} , and another is in the alignment of the acoustic array, both of

which can be kept within a few per cent.

Fluxatron

The second instrument used in this experiment is the fluxatron, the development of which was described in Chapter I. The version used in this experiment is similar in design to the one described by Hicks (1970). It differs from the previous designs primarily in the use of integrated circuits. It is capable of calculating the covariance of any two signals falling in a frequency band between approximately 10^4 Hz and 6×10^{-3} Hz. In this experiment the instrument was used to compute the covariance between temperature T, and vertical wind w. The fluxatron console is lightweight and easily portable (see Figure 3b). It operates from a ± 15 volt supply and consumes about two watts.

The vertical velocity sensor is a Gill propeller anemometer molded from foamed polystyrene, with the rotating shaft extended three inches beyond the plane of the blades to provide symmetry. It has a response time of 0.3 sec and a threshold speed of 0.3 m/sec. The manufacturer's calibration showed linear response for wind speed in terms of revolutions per minute, for wind speeds from 1.2 m/sec to 22 m/sec. Voltage output was calibrated against revolutions per minute to give a final calibration of 0.2 m/sec for 1.0 volt output, again linear over the wind speed range of 1.2 m/sec to 22 m/sec.

At wind speeds less than 1.2 m/sec the propeller response is not linear and this poses a serious calibration problem. The problem was accentuated in an experiment such as this where the vertical wind changed sign frequently and thus the propeller changed direction of rotation (see Figure 4). This resulted in frequent passes through the threshold velocity

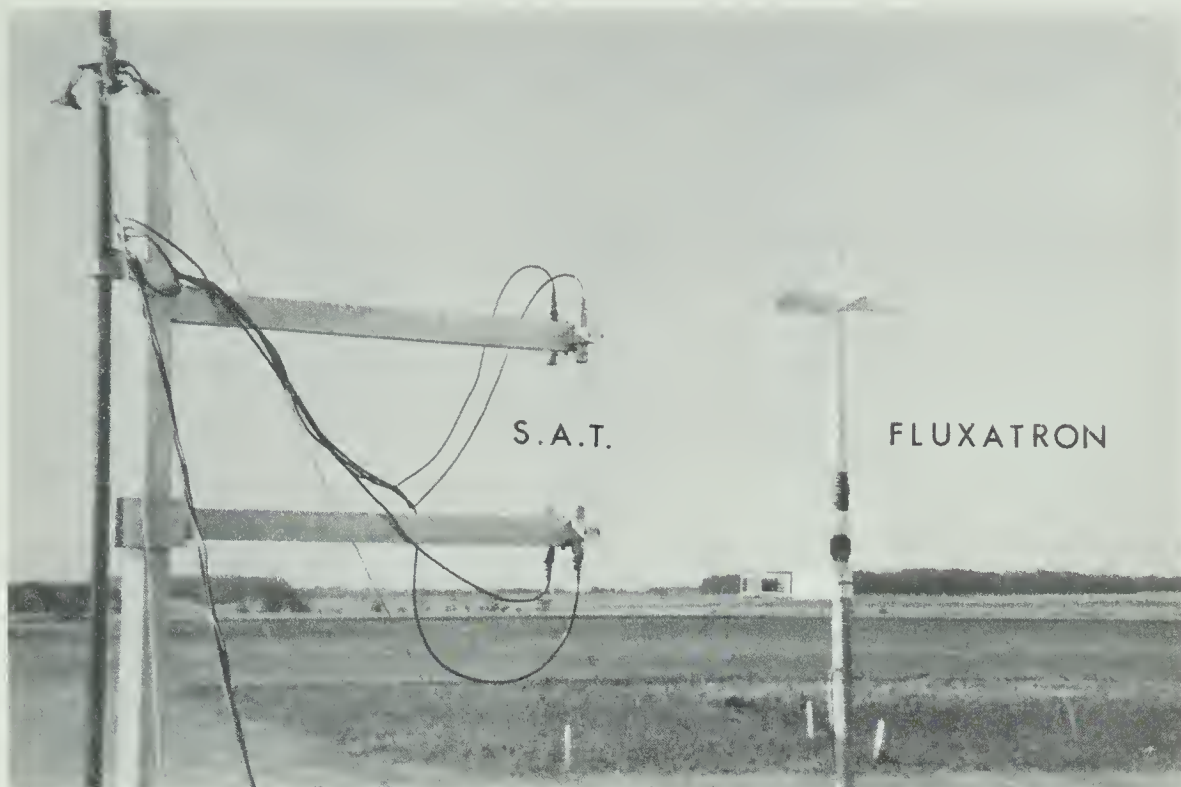


FIGURE 3a

Close-up photograph of the two sensor arrays.

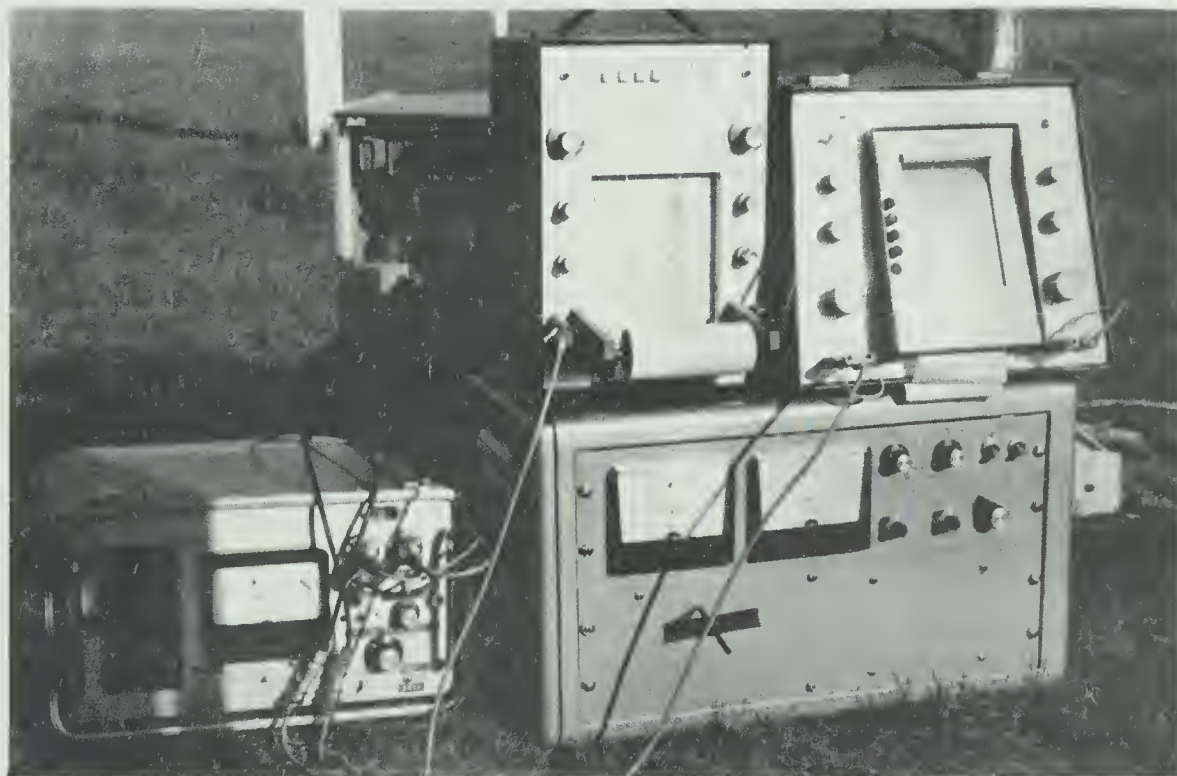


FIGURE 3b

Photograph of fluxatron console, S.A.T. console, and chart recorders.

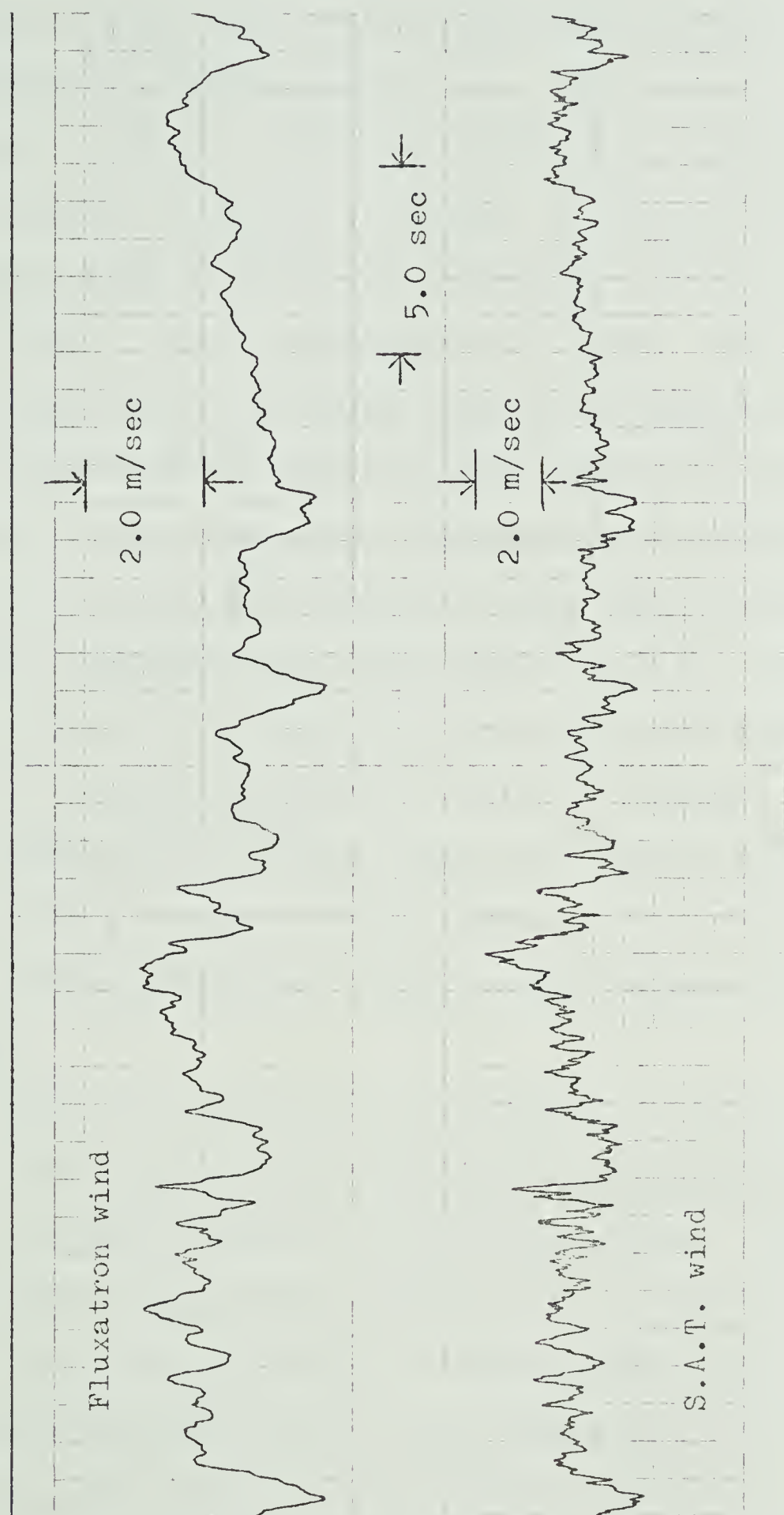


FIGURE 4

Comparative chart recorder traces of fluxatron vertical wind and S.A.T. vertical wind.

of ± 0.3 m/sec and in subsequent loss of response to low amplitude wind fluctuations. Figure 4 is a chart recorder trace of the vertical wind as measured by the fluxatron and the S.A.T. The time scale and the calibrations are shown. The limited high-frequency response of the fluxatron propeller anemometer is obvious. Of greater concern, however, was the large number of vertical wind fluctuations, both positive and negative, that are less in magnitude than 1.2 m/sec. These fluctuations were not within the linear response range of the anemometer, and, therefore, the calibration of these signals could not be determined accurately. For this reason, when calibrated for the linear response range, the fluxatron would be expected to give values of vertical wind fluctuations considerably lower than those of the S.A.T. That this is so, will be shown in the discussion of the results in a subsequent chapter.

The temperature sensor is a fine wire resistance thermometer made by wrapping .0013 cm diameter nickel wire around a plastic form. The wire response is linear, thus the calibration can easily be carried out in a controlled environment chamber to give temperature in terms of resistance.

During the construction of the fluxatron circuitry changes were made which left some doubt concerning the relation between the measured resistance of the wire and the output voltage. This portion of the circuitry has since been modified and so it is now impossible to check this facet of the calibration. The calibration which was made prior to the modification gave an output calibration of 1.5°C for 1.0 volt output, linear over the range of temperatures encountered.

In addition to the observations from the fluxatron and S.A.T., surface wind and temperature data were taken every hour at the Ellerslie

site. Also, hourly temperature data from two levels of the CN Tower in downtown Edmonton were used as an indication of boundary layer lapse rates throughout the experimental runs.

CHAPTER III

DATA COLLECTION AND REDUCTION

Data Collection

The fluxatron and the S.A.T. each measure the fluctuations in vertical wind and temperature, and hence there were four output signals to be recorded. These four signals were recorded simultaneously on magnetic tape and on paper strip charts. Two two-channel Brush chart recorders and a Precision Instrument seven-track FM magnetic tape recorder were used for the data collection. Numerous trial runs were made during July and August 1970 in order to check on the performance of the sensing and recording instruments. From these trial runs comparative measurements of w' and T' were made by analysis of the strip chart recordings. These trials and early analyses were necessary as a first check on the sensor calibrations and as guides for matching the output signal strengths to the dynamic range of the tape recorder. The trials were completed by the end of August at which time it was judged that the sensing and recording equipment was operating satisfactorily.

During the last week of August and the first week of September experimental runs were made which were to be used for complete analysis. Because of the calibration problem mentioned in Chapter II, only the runs of 6 September 1970 were subsequently considered suitable, and these data were used exclusively for the spectral analysis.

The time table for the experiment was to take six half-hour

runs in a four-hour period commencing at 10:18 MST (see Table 1). The tape recorder speed was $1 \frac{7}{8}$ inches per second, and with this speed the six half-hour runs were recorded on one 2400-foot tape. The four tape recorder channels used were individually calibrated in terms of sensor output by recording first a zero voltage signal, followed by a +2.0 volt signal and a -2.0 volt signal, each of approximately thirty seconds duration. These signals were generated by setting plus and minus 30° phase shifts on the S.A.T. 5 kHz frequency transmitter. The same signals were recorded on the two chart recorders as a check against chart paper calibration.

During the actual experiment the signals were recorded on the chart recorders as well as on the tape recorder. The chart recorders were used during the data collection as signal monitors, and the chart recorder data were later used for comparisons. After the six runs were completed, the magnetic tape signal was played back into the chart recorders, giving another set of data strip charts. These charts were compared to the monitor charts to identify any noise that may have been picked up during taping. The most dominant noise signal that could be identified visually was relatively high frequency. This noise was attributed to 60-cycle alternating current from the tape recorder power source. As the data were to be low-pass filtered prior to digitization, this noise was not considered a problem.

In addition to the data collection discussed above, temperature data from the CN Tower in the city centre of Edmonton are presented in Table 2 and were used as an indication of boundary layer lapse rates throughout the time period of the experiment.

TABLE 1

<u>TIMETABLE OF OBSERVATIONAL SAMPLES 6 SEPTEMBER 1970</u>						
RUN NO.	1	2	3	4	5	6
BEGIN	10:18	11:00	11:40	12:20	13:00	13:42
TEMP (°F)	56.5	56.4	58.0	59.0	59.0	60.5
WIND (MPH)	NW 16	NW 18	NW 18	NW 20	NW 16	NW 14
SKY	3/10 CU	4/10 CU	4/10 CU	4/10 CU	2/10 CU	1/10 CU
END	10:48	11:30	12:10	12:50	13:30	14:20

TABLE 2

<u>TEMPERATURES AT 115 m AND 17 m</u> <u>ON THE CN TOWER IN EDMONTON</u>		
TIME (MST)	$T_{115m} - T_{17m}$ (°F)	T_{17m} (°F)
10:00	-2.6	55.3
11:00	-3.0	56.8
12:00	-2.9	57.8
13:00	-3.1	58.3
14:00	-2.9	58.9
15:00	-3.0	59.9

Analog to Digital Conversion

There are three general approaches to the analysis of analog signals. One is the use of an analog computer to analyze the data directly. This approach requires a fairly large computer for large amounts of data. The second involves hand digitization of the data with the obvious limitation being the amount of data that can be handled. The third approach, and the one used in this study, is an electronic analog-to-digital conversion (A/D), followed by analysis with a digital computer. In this case the computer used was the University of Alberta's IBM 360/67.

Immediately prior to conversion, the data were passed through low-pass filters with effective cutoff frequencies set at eighteen Hz to remove high-frequency noise.

Prior to A/D conversion, the desired frequency range had to be considered. The limits $10^{-3} \bar{u}/Z$ and $5\bar{u}/Z$ were used as guides to estimate the low and high frequencies, respectively, of the frequency interval which contains 95 per cent of the covariance. In this experiment $Z = 3.5$ m and $\bar{u} = 8$ m/sec which gave a desired frequency range of 2×10^{-3} to 10 Hz. The digitizing rate of the A/D converter used was 200/sec or 50/sec channel, with the four channels being digitized sequentially. The A/D converter was set up with two tape transports so that every second record or block would be recorded on one tape, and alternate records recorded on the other. This arrangement was used to avoid data loss at the inter-record gap. The data were digitized twice at two different tape playback speeds to attain the desired frequency range.

For the high-frequency end of the desired frequency range the data tape was digitized at the original recording speed of 1 7/8 inches

per second in blocks of length 2048 data points. The high-frequency limit to this subrange was determined by the Nyquist or folding frequency f_N , which is defined as $f_N = \frac{1}{2\Delta t} = \frac{1}{2} \times \frac{1}{1/50} = 25$ Hz. Above this frequency aliasing could be expected. However, in this case the analog signals were filtered above 18 Hz so that the effective high-frequency limit to this subrange was 18 Hz rather than the Nyquist frequency of 25 Hz. If a minimum sample length of one block were to be used for analysis, the sample length would be $2048/50 = 41$ sec. Since it is usually considered that a minimum of six cycles are required for spectral analysis, then the low frequency limit for this high frequency subrange would be $6/41$, or approximately 0.14 Hz. Therefore, the total frequency range which could be analyzed using a playback speed of $1 \frac{7}{8}$ inches per second was approximately 0.14 to 18 Hz.

This frequency range includes the high frequency objective of 10 Hz but does not approach the desired low frequency limit of 2×10^{-3} Hz. Therefore, in order to cover the low frequency end of the spectrum the tape was digitized a second time at a playback speed of 30 inches per second, which was 16 times the original recording speed. This high speed playback gave an effective filter cutoff of $18/16$ or approximately 1.1 Hz. The Nyquist frequency in this case was $25/16$ or approximately 1.6 Hz and thus the high frequency cutoff for this subrange was approximately 1.1 Hz as determined by the low pass filter. The time interval between digitized values was now $16/50$ sec and the length of one block was $2048 \times (16/50) = 655$ sec. Again, requiring a minimum of six cycles on which to base analysis, the low frequency limit became $6/655$, or approximately 10^{-2} Hz.

Digitizing twice gave data that could be analyzed over a frequency range of 10^{-2} to 18 Hz. During the analysis, which is to be

discussed in a subsequent chapter, the two sets of digitized data were used, with the emphasis placed on the analysis of the low frequency subrange of 10^{-2} to 1.1 Hz as this range contained all of the spectral peaks and a large percentage of the total variances and covariances. It should be noted that this digitizing procedure produced approximately 2.3×10^6 data points.

After digitization the two digital tapes with alternating blocks were copied onto one nine-track computer tape with the blocks ordered sequentially, and hence in a form ready for analysis. Prior to analysis, the digitized values were plotted using the Computing Centre's Calcomp plotter. These plots provided a visual check on the digitizing as they could be compared to both the monitor traces from the chart recorders and the playback traces of the analog signals from the FM tape recorder. They showed the effect of the filtering on the high frequency noise and provided a means of data selection for analysis. During the A/D conversion, a few high amplitude extraneous noise spikes appeared, apparently from minor power surges, and the plotted values provided a means of avoiding these during analysis.

The final step in the data preparation was the calibration of the digitized values. This was done by digitizing and subsequently plotting the 30° 5 kHz phase shifts, which, as mentioned earlier, are equivalent to 2.0 volts output. The determination of the digital range of these known signals, together with the sensor calibrations gave final calibrations to the digitized values. For the S.A.T. the calibrations were 3.69 m/sec and 6.25°C , each equivalent to 100 digits; and for the fluxatron they were 0.4 m/sec and 3.0°C , each equivalent to 100 digits.

CHAPTER IV

SPECTRAL ANALYSIS

The analysis of the digitized, calibrated data consisted first of computing the variance spectra of vertical wind and temperature, and the cospectrum between wind and temperature, using the data from the two sensing instruments. Secondly, comparative heat fluxes were calculated from the cospectrum of w' and T' as measured by each instrument, and by computing the covariances of the digitized w' and T' data from the two instruments.

The techniques of spectral analysis have been developed and discussed by Blackman and Tukey (1958) and Jenkins (1961). More recently, the major change in technique has been the development of the "fast" Fourier transform (FFT) described by Cochran et al (1967) and Bingham, Godfrey and Tukey (1967).

The procedure used in this thesis was to compute the Fourier coefficients using an FFT, and from these to compute the spectra and cospectra. The FFT subroutines used were supplied by the University of Alberta, Geophysics Division, Department of Physics, and adapted for use with the wind and temperature data collected in this experiment. When the computer program was ready for use in analysis, it was tested by performing spectral analysis on perfect sine waves of known frequencies and amplitudes. When it was considered that the program was performing correctly, the data analysis was begun.

Briefly, the analysis consisted of reading the data from magnetic tape, removing the mean and any linear trends to give the fluctuations, calibrating these fluctuations, computing the Fourier coefficients, and finally, computing the spectral estimates.

The spectral estimates were then smoothed using a Parzen lag window. This smoothing technique was chosen primarily because it maintains the sample coherence function between its theoretical values of ± 1 ; whereas the Hanning lag window allows the sample coherence function to vary over wider limits.

Eventually, the program was developed to where it computed the spectra of wind and temperature for both the S.A.T. and the fluxatron, the cospectrum between wind and temperature for each instrument, the summed variances and covariances, the quadrature spectra, and the coherence. It also plotted these results in both absolute and normalized form using the Computing Centre's Calcomp plotter.

CHAPTER V

DISCUSSION OF RESULTS

As mentioned previously, the analysis of the data consisted primarily of calculating spectra and cospectra of temperature and vertical wind fluctuations. Heat fluxes were then derived from the cospectra and compared to heat fluxes calculated from the covariances of the digitized data.

The results presented here are based on calculations made on data collected on 6 September 1970, between the times of 10:18 and 14:20 MST. It was a cool day, with fairly brisk northwest winds and a few tenths of small cumulus (see Table 1). Hourly temperature data were collected from two levels of the CN Tower in Edmonton as an indication of low-level lapse rates during the experimental runs (see Table 2). During the times of the experimental runs the lapse rate averaged 2.9°F between the two levels 98 m apart, with a maximum deviation from this mean of only 0.3°F . This is equivalent to a lapse rate of $1.7^{\circ}\text{C}/100\text{ m}$ or to a Richardson number of -0.03 . Since the dry adiabatic lapse rate is $0.98^{\circ}\text{C}/100\text{ m}$, this indicated quite pronounced instability throughout the first 100 m of the surface boundary layer.

Coherences

As an indication of the high frequency limit to which the independently computed spectra might be expected to show agreement, the coherences between the two wind and two temperature signals were computed.

The coherence between two variables is a measure of the relationship between them for various periods, and is analogous to a correlation coefficient which is a function of frequency.

In this case the coherence between the S.A.T. wind and fluxatron wind was calculated over the low frequency range (see Figure 5), and over the high frequency range (see Figure 6) using sample sizes discussed in Chapter III. These two figures indicate quite high correlation between the two measured winds between .01 Hz and 1.0 Hz. The rapid decrease in coherence above 1.0 Hz was attributed to the high frequency limit of the propeller anemometer, and also to the separation of the two sensors. Although this separation was quite small (about 50 cm., see Figure 3a), eddies of higher frequency than 1.0 Hz were apparently not highly correlated at this cross wind separation. The extremely rapidly decreasing coherence shown in Figure 5 was also attributable to the effective filter cutoff frequency of 1.1 Hz used in the low frequency analyses. The high frequency coherence analysis (Figure 6), shows a rapidly increasing signal correlation above 5.0 Hz. Since these frequencies were well above the response of the propeller anemometer, this correlation was between the system noises which were superimposed on the individual signals, and in this frequency range were of greater magnitude than the signals themselves.

Coherences between the two temperature signals were computed in a similar manner to those between the two winds. The low frequency range of temperature coherence is shown in Figure 7, and the high frequency coherence in Figure 8. The results are similar to those of the winds except for the influences of sensor responses. The two figures indicate quite high correlation between the two temperature signals over

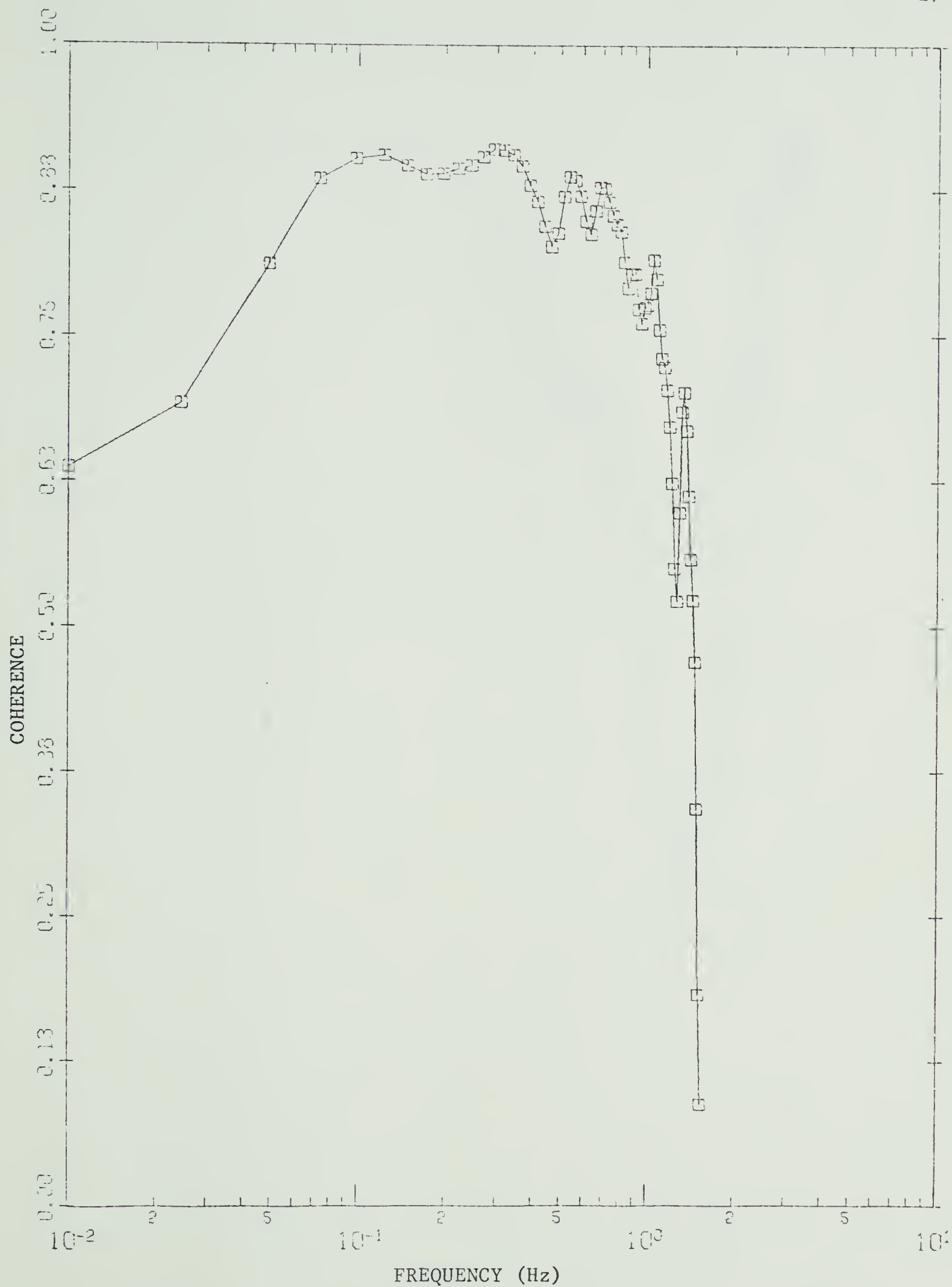


Figure 5 Coherence between S.A.T. wind and fluxatron wind over the low frequency range of analysis.

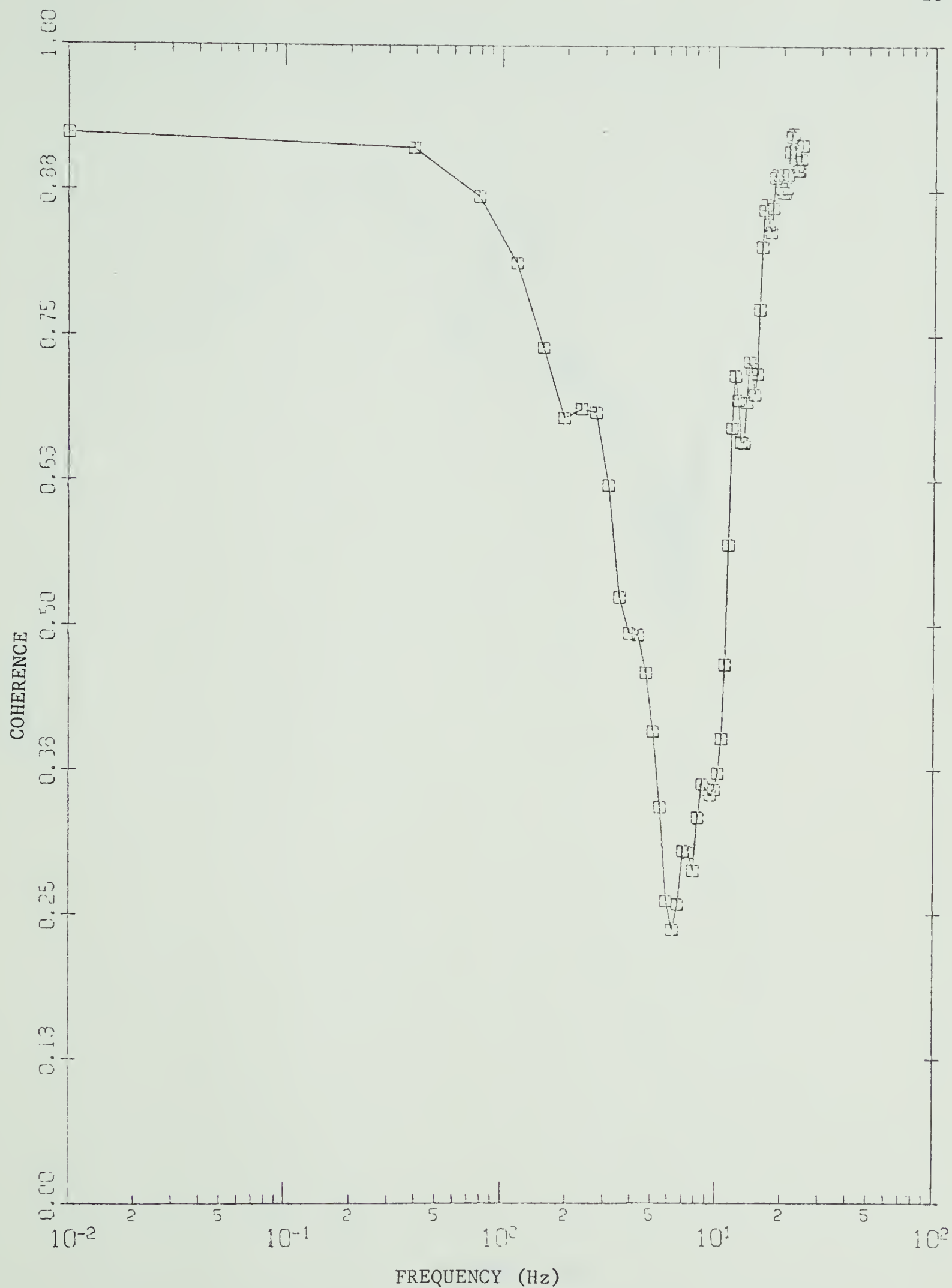


Figure 6 Coherence between S.A.T. wind and fluxatron wind over the high frequency range of analysis.

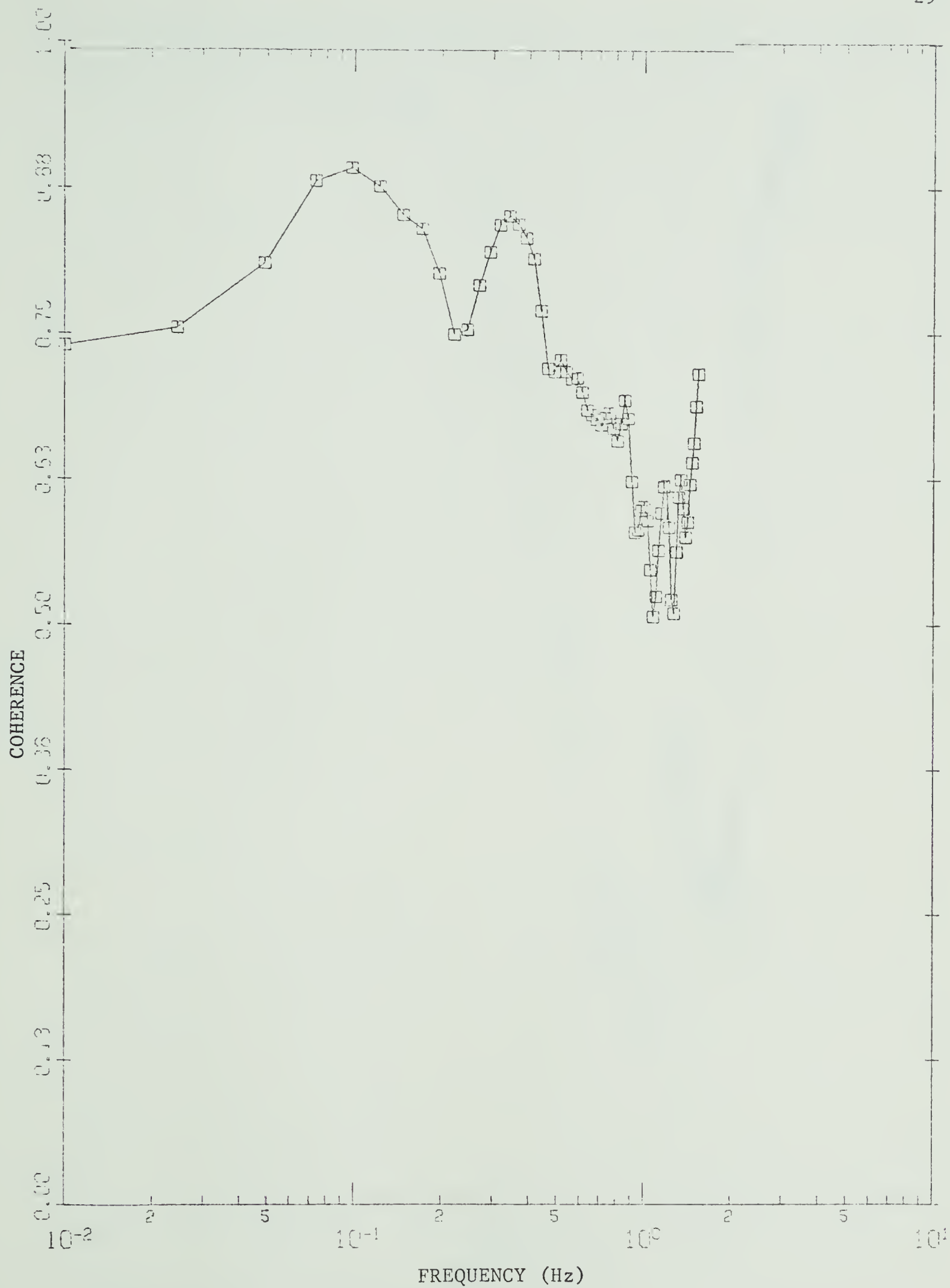


Figure 7 Coherence between S.A.T. and fluxatron temperatures over the low frequency range of analysis.

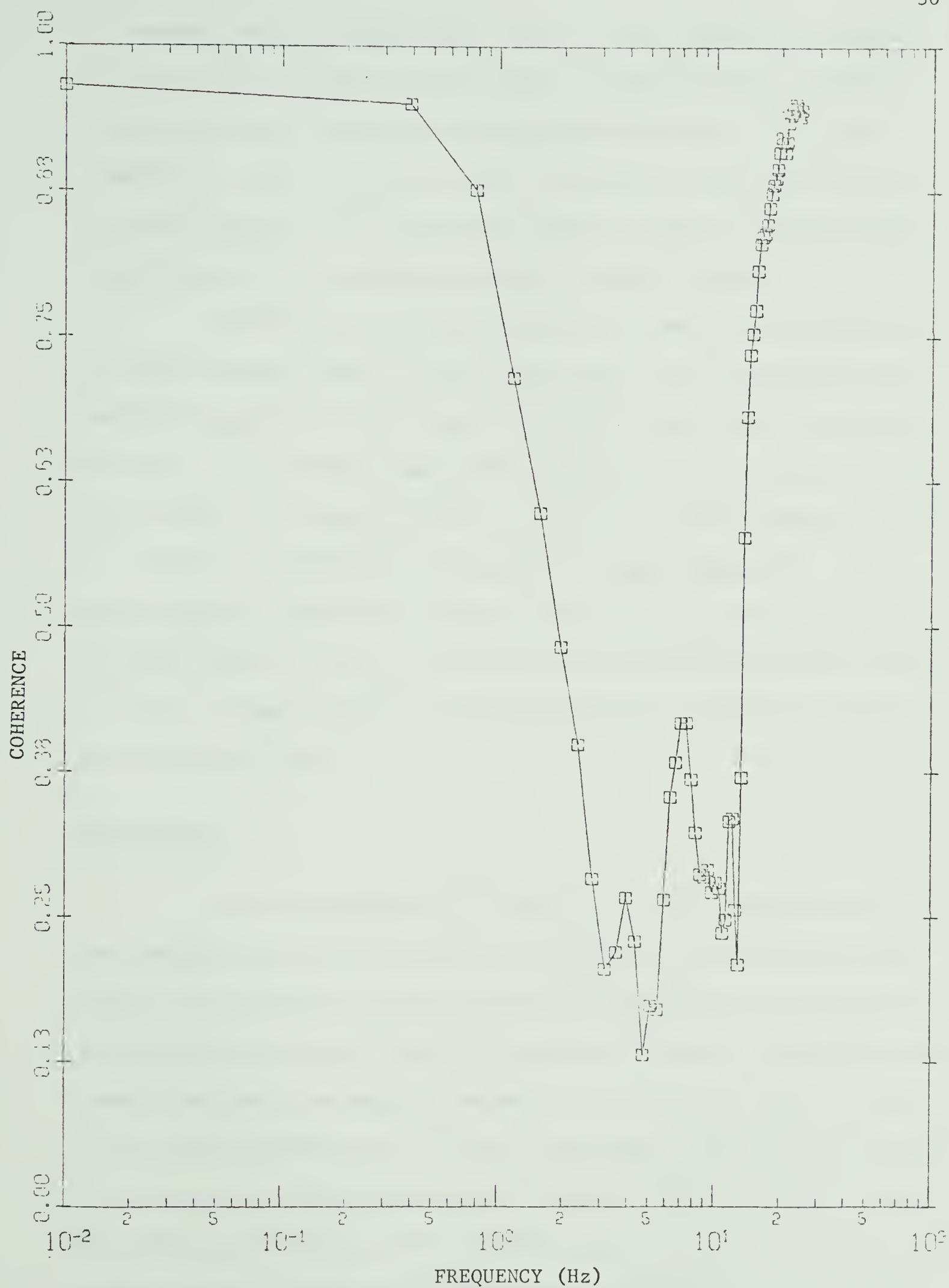


Figure 8 Coherence between S.A.T. and fluxatron temperatures over the high frequency range of analysis.

a frequency range of approximately .01 to 0.5 Hz. Since the analyses of both frequency ranges showed a fairly rapidly decreasing coherence beginning at about 0.5 Hz, this was again attributed to the sensor separation. Also, as with the winds, the rapidly increasing coherence at high frequencies was a correlation between signals of system noise which were on all the channels and were of small amplitude.

The foregoing coherence analyses were made as an indication of the high frequency limit at which comparisons can be made between the individual spectra of heat fluxes. It appeared that above frequencies of about 0.5 Hz the two sensor arrays were not measuring the same eddies, or at least not the same portion of an eddy. This high frequency cutoff is a function of horizontal wind speed and sensor separation. The optimum sensor separation would be a distance that is just large enough to insure that the sensors themselves do not interfere with each other's air flow, yet small enough to give high frequency correlation between the two output signals.

Wind Spectra

The variance spectra of vertical wind were calculated for the two frequency ranges and plotted in both absolute and normalized form. Figure 9 is an example of the absolute variance spectra calculated from the vertical wind data of the S.A.T. and the fluxatron. The square plot symbols represent the spectral estimates from the S.A.T. data and the round symbols represent the fluxatron estimates. Plotted in this manner, with frequency against frequency times spectral density, the area under the curve represents the total variance, and the area under the curve between any two frequencies represents the variance contribution from

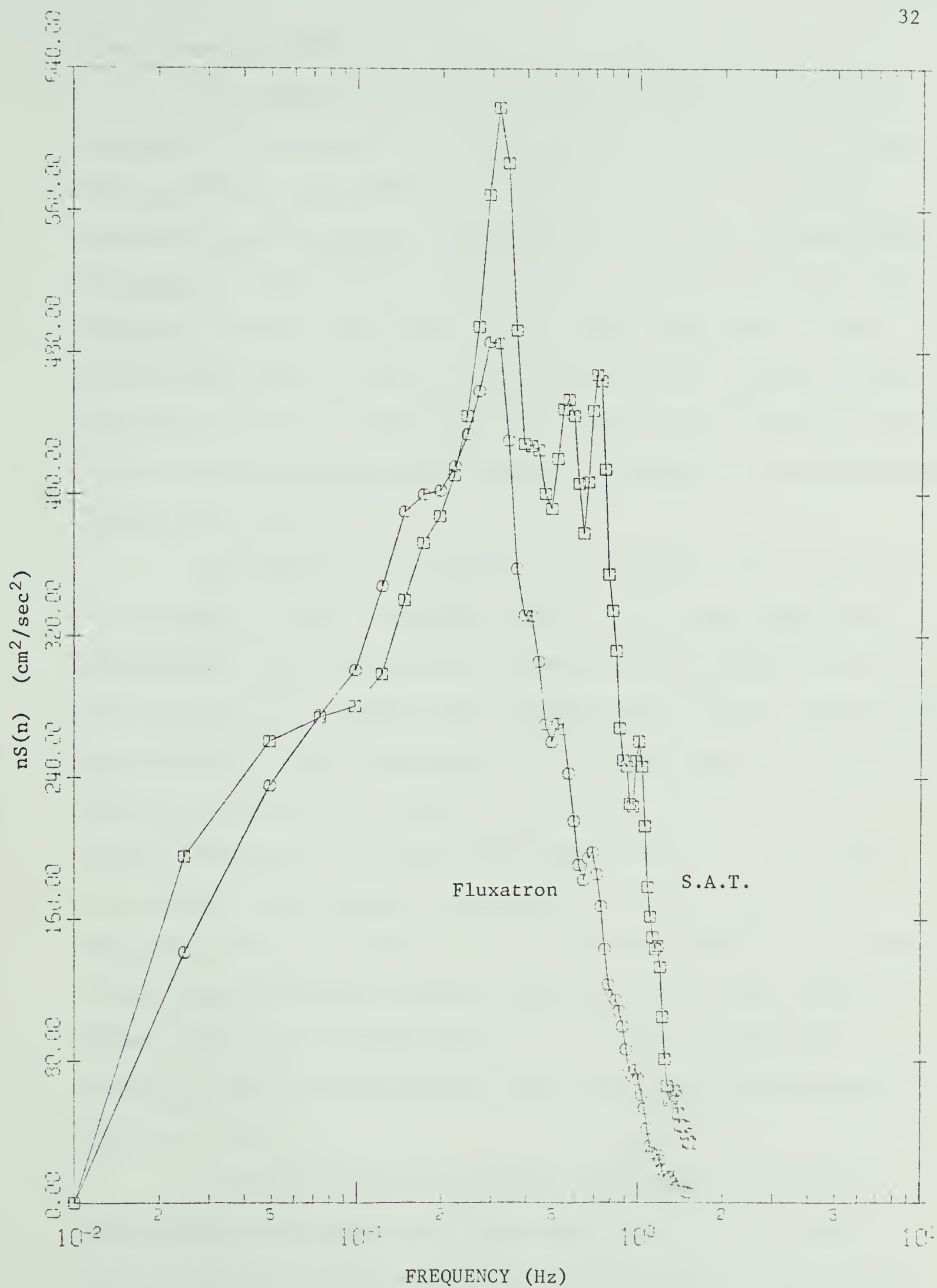


Figure 9 Absolute variance spectra of vertical wind over the low frequency range of analysis.

that frequency interval.

The analyses of the two instruments' data showed excellent agreement on the position of the variance peak on the frequency scale, which in this case was slightly above 0.3 Hz. Most of the published results in this field express frequency in terms of the non-dimensional frequency f . This quantity is defined as $f = nZ/\bar{u}$, where n is the real frequency in cycles per second, Z is the height above ground of the observations, and \bar{u} is the mean wind at that height. In this experiment the height Z was 3.5 m and \bar{u} was 7.7 m/sec (from data of Table 1). Hence, in this case the variance peak of vertical winds was at a non-dimensional frequency of 0.13.

This value seemed reasonable when compared to the results of other authors. Lumley and Panofsky (1964, p. 167), when summarizing experimental results, note that the variance peak was usually between 0.1 and 0.6 on the non-dimensional frequency scale, and that the spectral peak shifted to higher frequencies with increasing stability. Busch and Panofsky (1968) found the maximum variance at $f = 0.3$ for unstable cases. Sitaraman (1970) found a much lower value of $f = .01$ for the spectral peak and attributed this result to variable cloud cover. Zubkovskiy and Koprov (1969) also reported vertical wind variance maxima at much lower frequencies than most authors. A more recent report by McBean (1971) gave a variance peak at $f = 0.2$ for unstable cases. Pond et al (1971) reported similar results over water with the spectral peak at $f = 0.3$.

The magnitudes of the variance peaks and the comparative areas under the two curves were consistently lower for the fluxatron than for the S.A.T. This was a result of the instrument calibrations.

As was mentioned earlier, the propeller anemometer response is non-linear at wind speeds less than 1.2 m/sec. Since the vertical velocity fluctuations were of this order of magnitude, the calibration of the output signals was uncertain. Summed variances were computed from the digitized data (see Table 3) in order to assess the effect of this non-linearity of response. The variances were converted to standard deviations of vertical wind and the ratios of the standard deviations from the two instruments were computed. The S.A.T. fluctuations were, on the average, 31 per cent higher than the fluxatron fluctuations, with the percentage ranging from 16 to 43. This variation would be expected to be dependent upon the magnitude of the vertical wind fluctuations and, hence, also upon stability.

Figure 10 is a high frequency analysis of the absolute variance spectra of the vertical wind. The position of the variance peaks do not agree as closely in this case, because of the lack of statistical significance of the low frequency points in this higher frequency analysis. Of interest in this case is the high frequency end of the spectra, which shows a more pronounced variance dropoff for the fluxatron than for the S.A.T., attributable to the limited response of the propeller anemometer.

Figures 11 and 12 are normalized variance spectra of vertical wind. They are based on the same data as the absolute spectra of Figures 9 and 10, and are normalized by dividing the spectral estimates by the total variance, as computed from the digitized data. They are then plotted as the logarithm of frequency against the logarithm of normalized spectral density.

Defining an atmospheric inertial subrange as a range of eddy

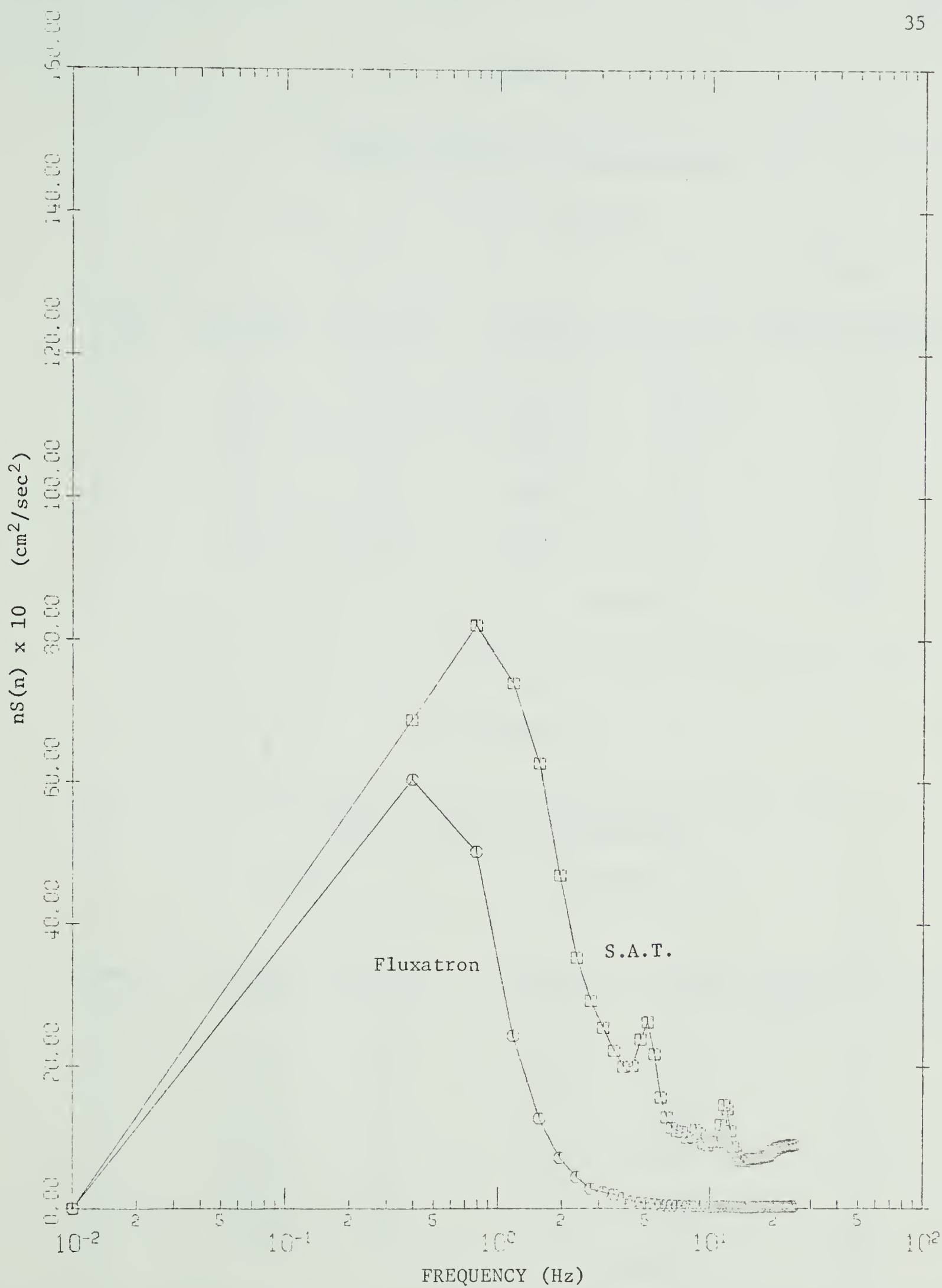


Figure 10 Absolute variance spectra of vertical wind over the high frequency range of analysis.

TABLE 3

<u>SUMMED VARIANCES OF VERTICAL WIND</u>					
S.A.T.			FLUXATRON		RATIO
Sample No.	Variance (cm ² /sec ²)	STD. Dev. (cm/sec)	Variance (cm ² /sec ²)	STD. Dev. (cm/sec)	<u>STD. Dev. S.A.T.</u> <u>STD. Dev. Fluxatron</u>
1	3905	62.5	1925	43.8	1.43
2	3850	61.9	2352	48.5	1.28
3	3982	63.0	1881	43.3	1.45
4	3254	57.0	2055	45.3	1.25
5	3947	62.8	2469	49.7	1.26
6	3125	56.8	2375	48.7	<u>1.16</u>
AVERAGE					1.31

TABLE 4

<u>SUMMED VARIANCES OF TEMPERATURE</u>					
S.A.T.			FLUXATRON		RATIO
Sample No.	Variance (°C) ²	STD. DEV. (°C)	Variance (°C) ²	STD. DEV. (°C)	<u>STD. DEV. S.A.T.</u> <u>STD. DEV. Fluxatron</u>
1	0.41	0.64	0.25	0.50	1.28
2	0.30	0.55	0.30	0.55	1.00
3	0.40	0.63	0.52	0.72	0.88
4	0.50	0.71	0.38	0.62	1.14
5	0.35	0.59	0.49	0.70	0.84
6	0.32	0.58	0.52	0.72	<u>0.81</u>
AVERAGE					0.99

sizes which are small enough to be isotropic, yet large enough to be unaffected by viscosity, Kolmogorov presented the hypothesis, that in this range the spectrum is a function of dissipation of energy per unit mass and of frequency only. Priestley (1959, p. 59) and Lumley and Panofsky (1964, p. 83) discussed the inertial subrange in relation to observed results. By dimensional analysis it can be shown that $S(n) = \alpha \epsilon^{2/3} n^{-5/3}$ where $S(n)$ is spectral density, ϵ is the rate of energy dissipation, n is frequency, and α is a universal constant. Hence, by plotting the normalized spectral estimates in logarithmic form this relationship can be tested by computing slopes. This relationship is referred to as the "minus five-thirds power law", or "Kolmogorov power law".

Figure 11 shows normalized spectra of vertical wind over the low frequency range of analysis. The square plot symbols represent analyses of the S.A.T. data, the round symbols of the fluxatron data, and the solid straight line has a slope of $-5/3$. The two plotted curves appear to fit the $-5/3$ slope fairly well between approximately 0.3 Hz and 1.0 Hz. This is the maximum range over which such a fit could be expected in this case. At frequencies near 0.3 Hz, energy is fed in from the shear, and in or out from the temperature gradient (depending on whether conditions are stable or unstable) and hence, the spectrum is anisotropic. At frequencies above 1.0 Hz the low pass filtering resulted in quite rapid dropoff of both curves.

Pond, Stewart, and Burling (1963) have derived an approximate criterion for isotropy in the boundary layer. This is that $n > 4.5\bar{u}/2\pi Z$, where n is frequency, \bar{u} is the mean wind speed and Z is the height of observation. In the present experiment $\bar{u} = 7.7$ m/sec and Z is 3.5 m which gives a limiting value for n of 1.6 Hz. At

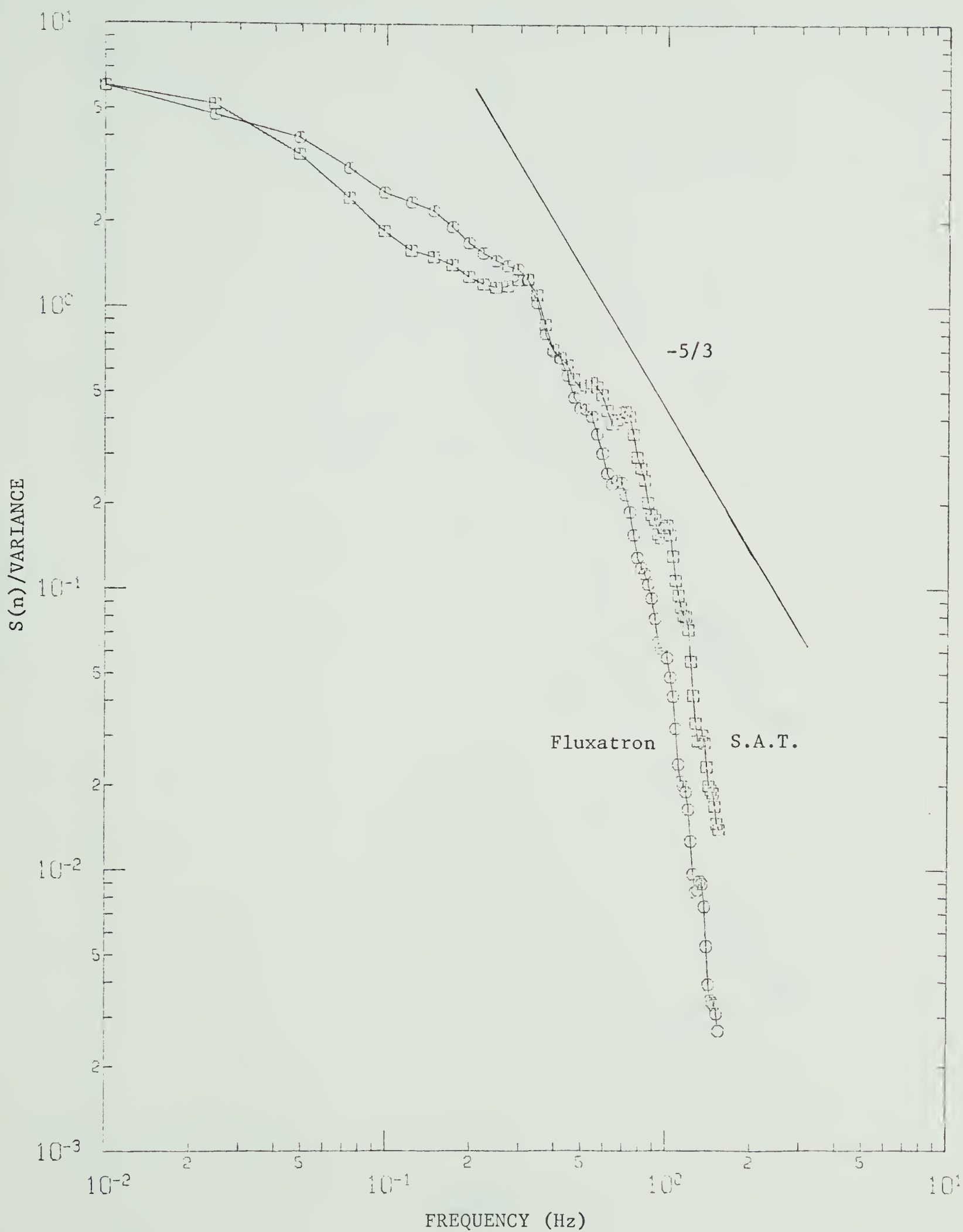


Figure 11 Normalized variance spectra of vertical wind over the low frequency range of analysis.

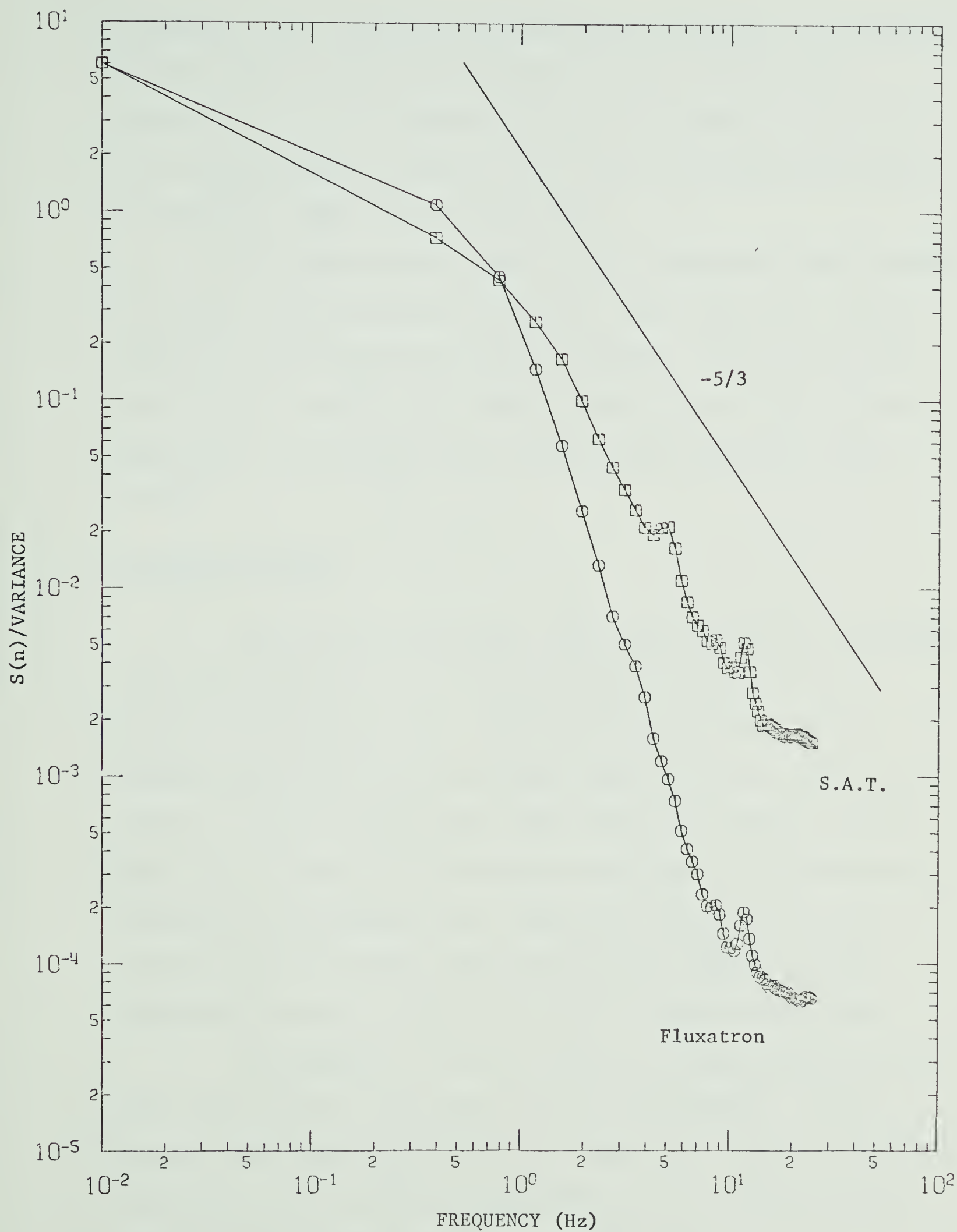


Figure 12 Normalized variance spectra of vertical wind over the high frequency range of analysis.

frequencies lower than this the eddies are not expected to be isotropic, and the $-5/3$ law would not be expected to hold. In the present experiment the $-5/3$ law appeared to hold at frequencies as low as 0.3 Hz. This interesting extension of the $-5/3$ law has been noted earlier by Pond et al (1966) and MacCready (1953).

The high frequency analyses of the normalized variance spectra of vertical wind are plotted in Figure 12. Again the S.A.T. results (square plot symbols) showed excellent agreement with the $-5/3$ slope above 0.3 Hz. Because of the limited response time of the propeller anemometer, the fluxatron results showed a much steeper slope above 1.0 Hz.

Temperature Spectra

As with the vertical wind, the variance spectra of temperature were calculated for the two frequency ranges and plotted in both absolute and normalized form. Figure 13 is a plot of the absolute variance spectra for the low frequency range. The S.A.T. (square plot symbols) and the fluxatron agree well in this case, giving a spectral peak in the vicinity of 0.04 Hz which corresponds to a non-dimensional frequency of approximately 0.02. This result agreed well with the results obtained by McBean (1971) who found the spectral peak for temperature between $f = 0.02$ and $f = 0.03$ for unstable conditions.

The magnitude of the two temperature variance peaks and the areas under the two curves were in quite close agreement. Table 4 compares summed variances for the six samples. For individual samples the range of the variations was about ± 20 per cent, but the average ratio of the two summed variances was nearly unity.

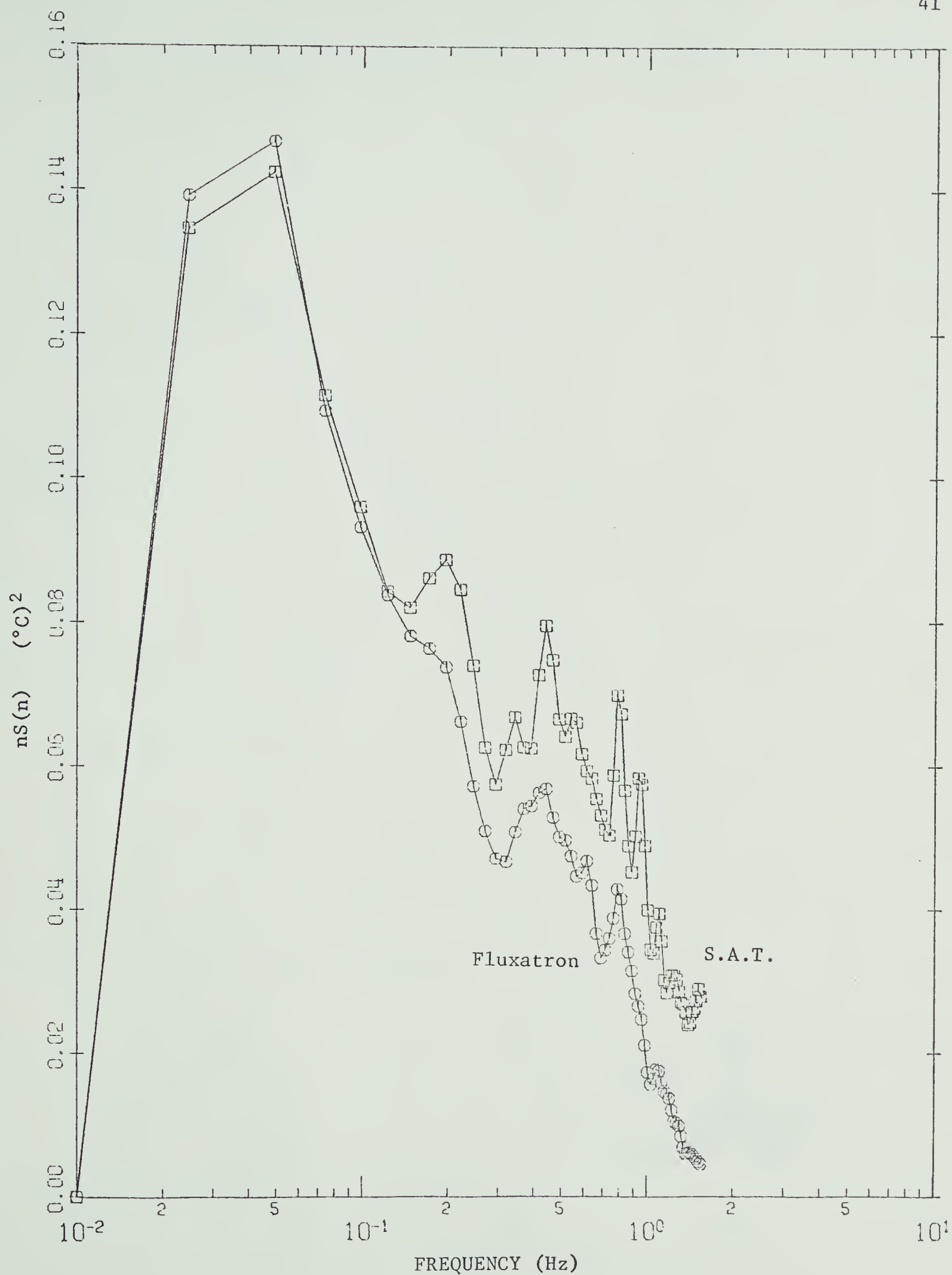


Figure 13 Absolute variance spectra of temperature over the low frequency range of analysis.

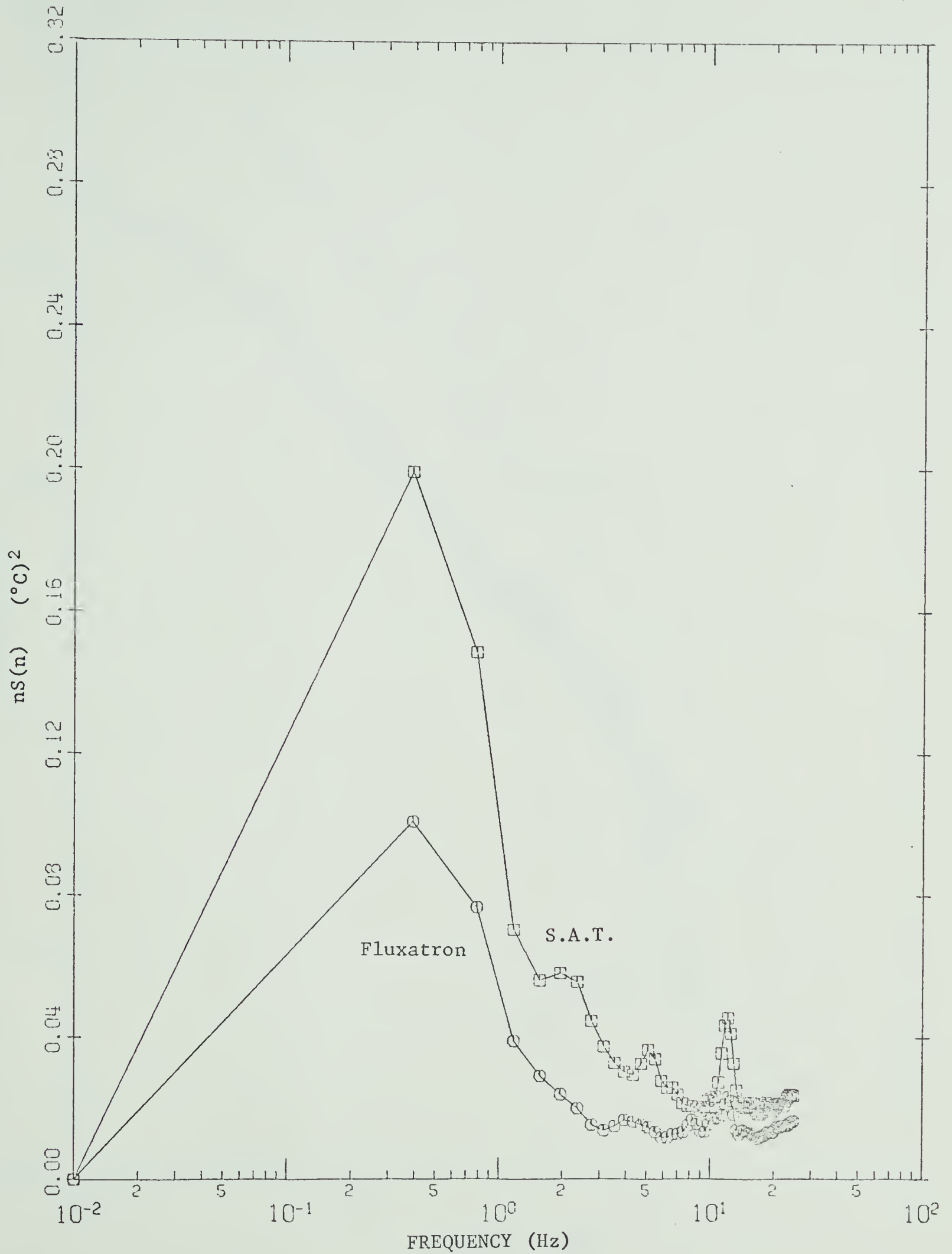


Figure 14 Absolute variance spectra of temperature over the high frequency range of analysis.

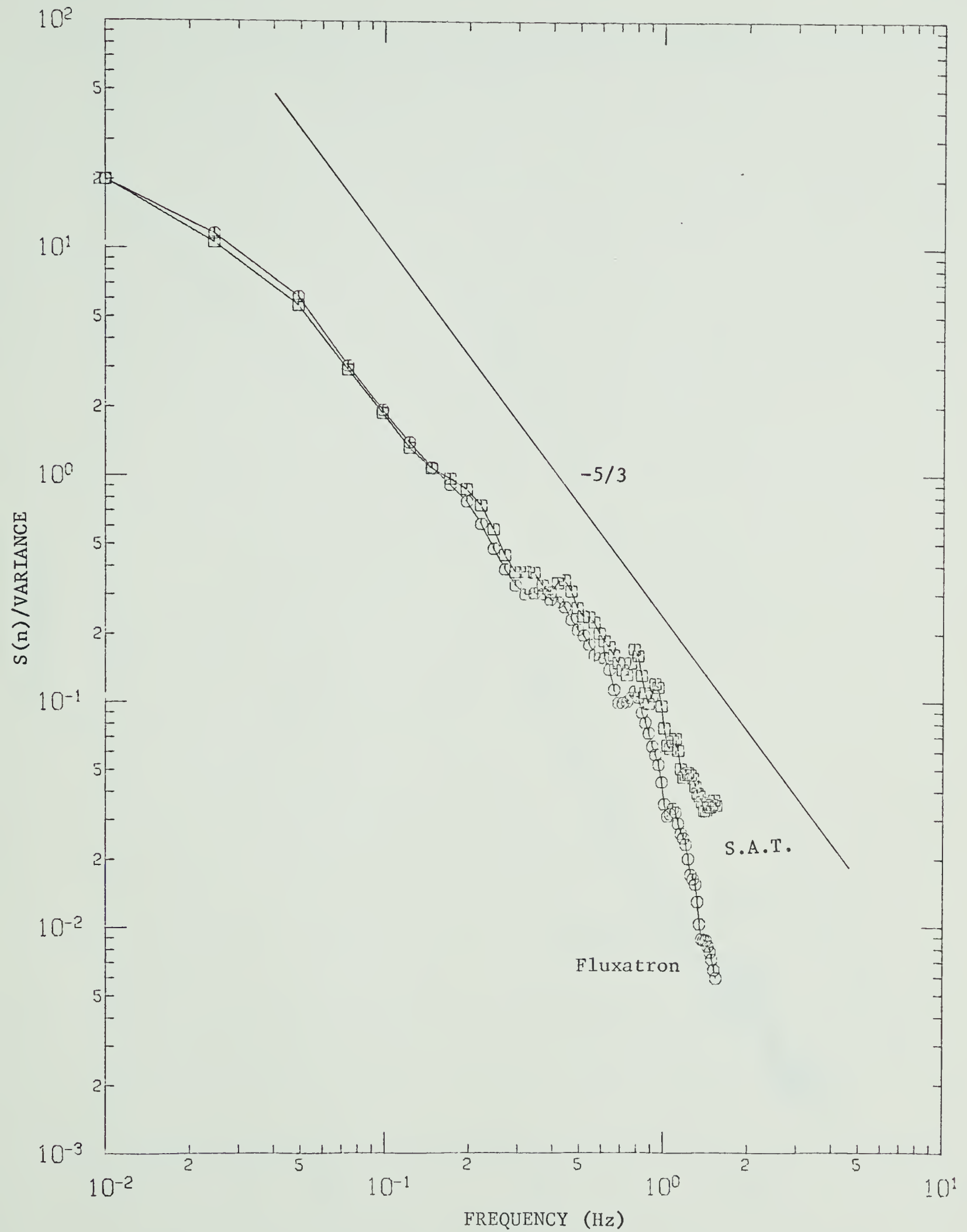


Figure 15 Normalized variance spectra of temperature over the low frequency range of analysis.

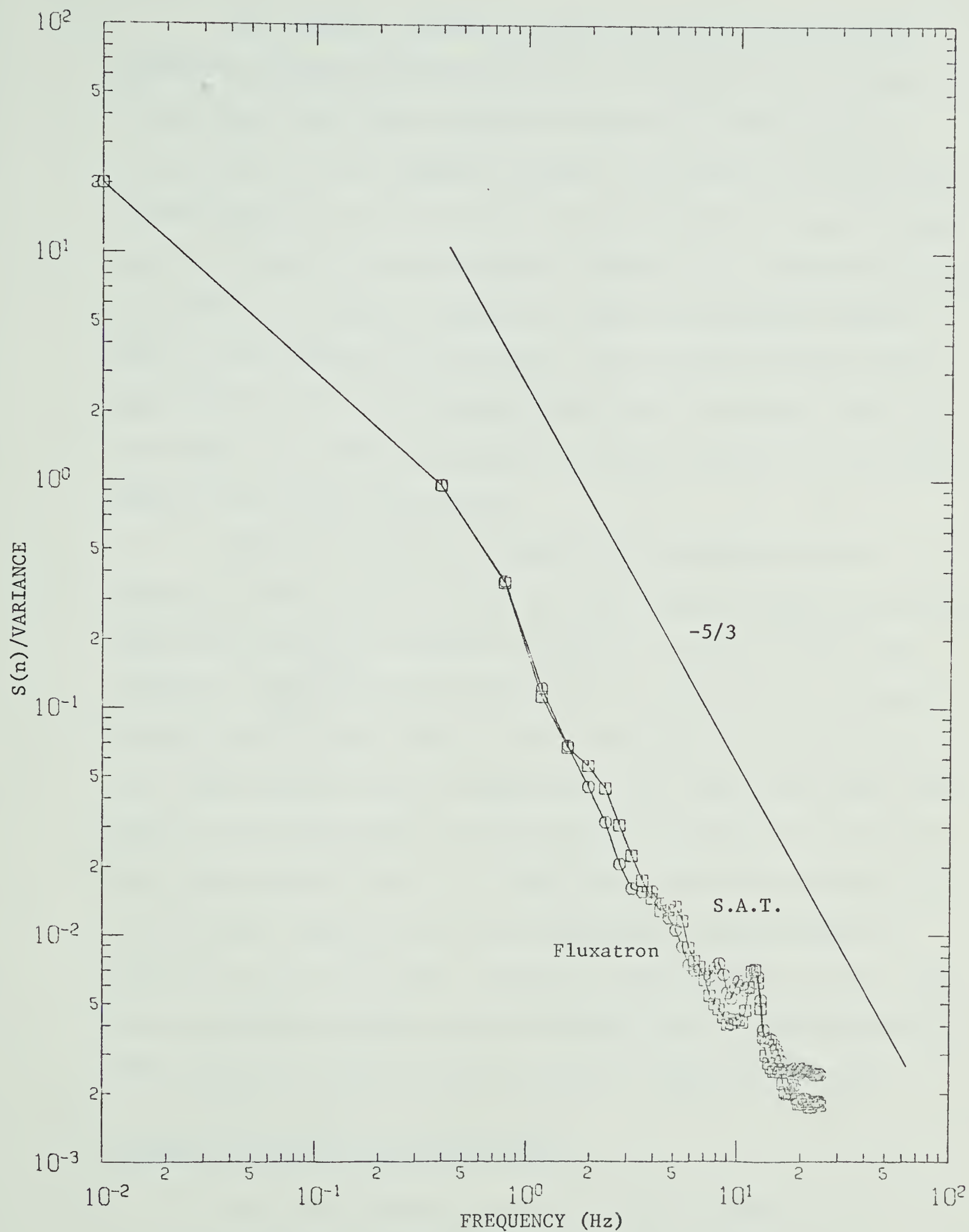


Figure 16 Normalized variance spectra of temperature over the high frequency range of analysis.

The absolute variance spectra of temperature for the high frequency range are plotted in Figure 14. The positions of the peak in this figure were quite unreliable because the actual position of the peak from the low frequency analysis (see Figure 13) was much below the low frequency cutoff of 0.14 Hz, as determined by the sample lengths used for the high frequency analysis. Elsewhere, over the high frequency range, the two instruments appeared to make quite comparable measurements of the temperature fluctuations. The secondary spectral peak of approximately 12 Hz on the frequency scale was an extraneous peak (see also Figure 10), which is believed to have been generated by the capstan drive of the analog tape recorder.

Figures 15 and 16 are plots of the normalized variance spectra of temperature for the low and high frequency ranges, respectively. They were normalized by dividing the spectral estimates by the total variance of temperature as computed from the digitized data. As noted by Lumley and Panofsky (1964, p. 85), an inertial subrange also exists for a scalar quantity such as temperature, and a "minus five-thirds law" applies to the temperature spectrum as well as to that of the vertical wind. From Figures 15 and 16 it appears that the spectra followed the $-5/3$ law quite closely over the non-dimensional frequency range of $f = 0.02$ to the filter cutoff frequency at approximately $f = 8.0$. Also the two sensing instruments agreed very well except at high frequencies, where the sensor separation caused dissimilar sample fluctuations.

Cospectra Between Wind and Temperature

One of the primary objectives of this experiment was to compute comparative cospectra between wind and temperature using a

S.A.T. and a fluxatron as sensing instruments. These comparative cospectra were computed over the low frequency range only, because the covariance contribution from the high frequency range was small and could not be used for direct comparison because of the sensor separation.

Figures 17 to 20 are plots of the absolute cospectra with the ordinates calibrated in heat flux units, in this case milliwatts/cm². The plotting symbols used for the cospectral plots are reversed from those used with the individual wind and temperature spectra. Hence, the square plot symbols represent the analyses of the fluxatron data, and the round plot symbols represent the analyses of the S.A.T. data. Figures 17 to 20 are identical analyses of four different data samples. These examples were chosen to illustrate the large sample fluctuations. This point is further illustrated by Figures 17 and 18, based on data samples that were sequential in time. These large sample fluctuations indicate that the sample lengths chosen for analysis were too short to give highly representative cospectra. Miyake, Stewart and Burling (1970) made note of the same problem, when they mentioned that the integrated values of heat flux were much less reliable than those of momentum flux, because of the pronounced variability of cospectral estimates of heat flux.

Despite the large sample fluctuations the frequency of the cospectral peak is nearly stationary from sample to sample. This is to be expected because all of the samples were taken under nearly identical stability conditions. The mean position of this peak was at 0.09 Hz, which corresponds to a non-dimensional frequency of $f = 0.04$. This value is somewhat lower than that obtained by other authors.

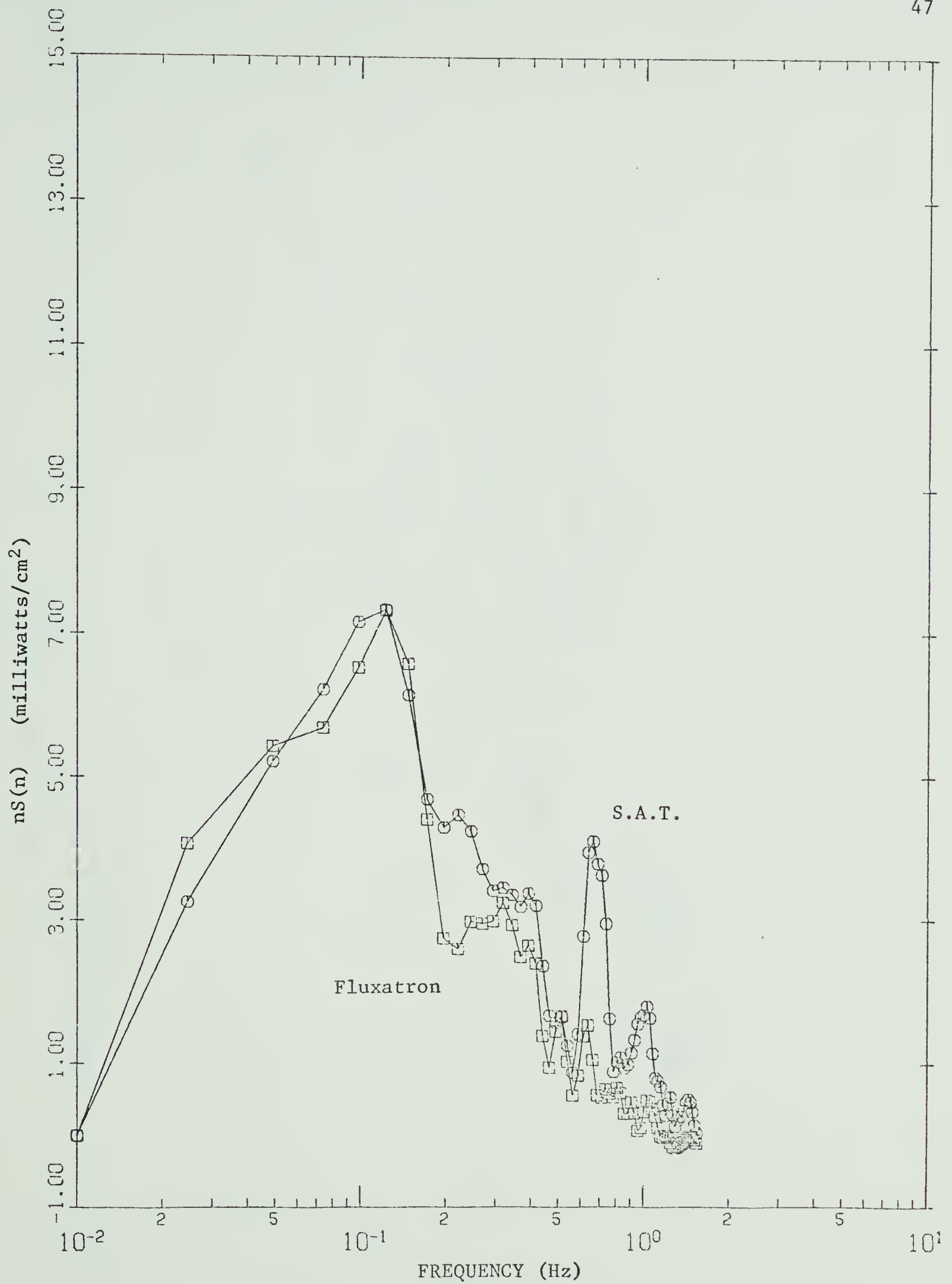


Figure 17 Absolute cospectra between wind and temperature over the low frequency range of analysis.

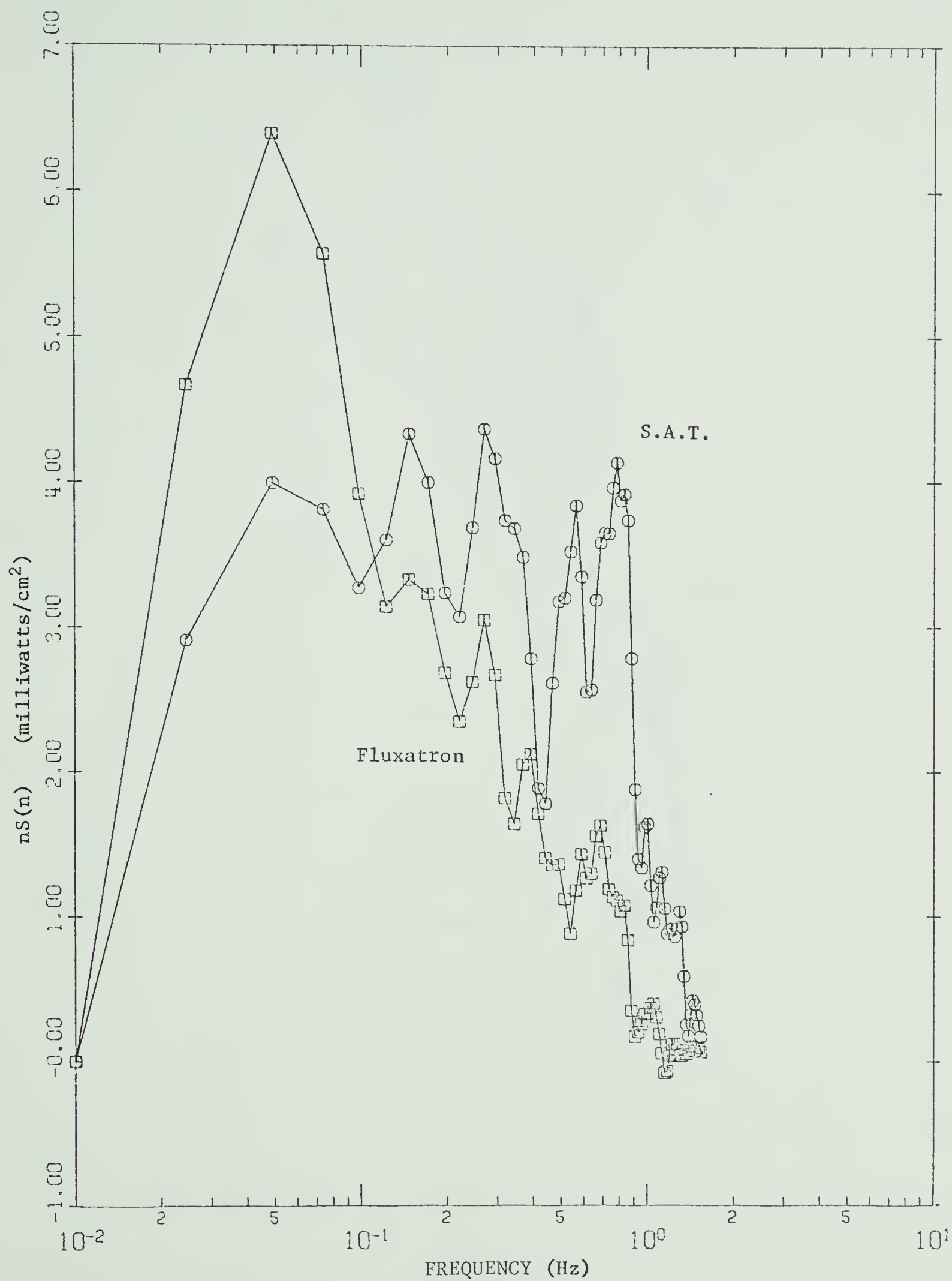


Figure 18 Absolute cospectra between wind and temperature over the low frequency range of analysis.

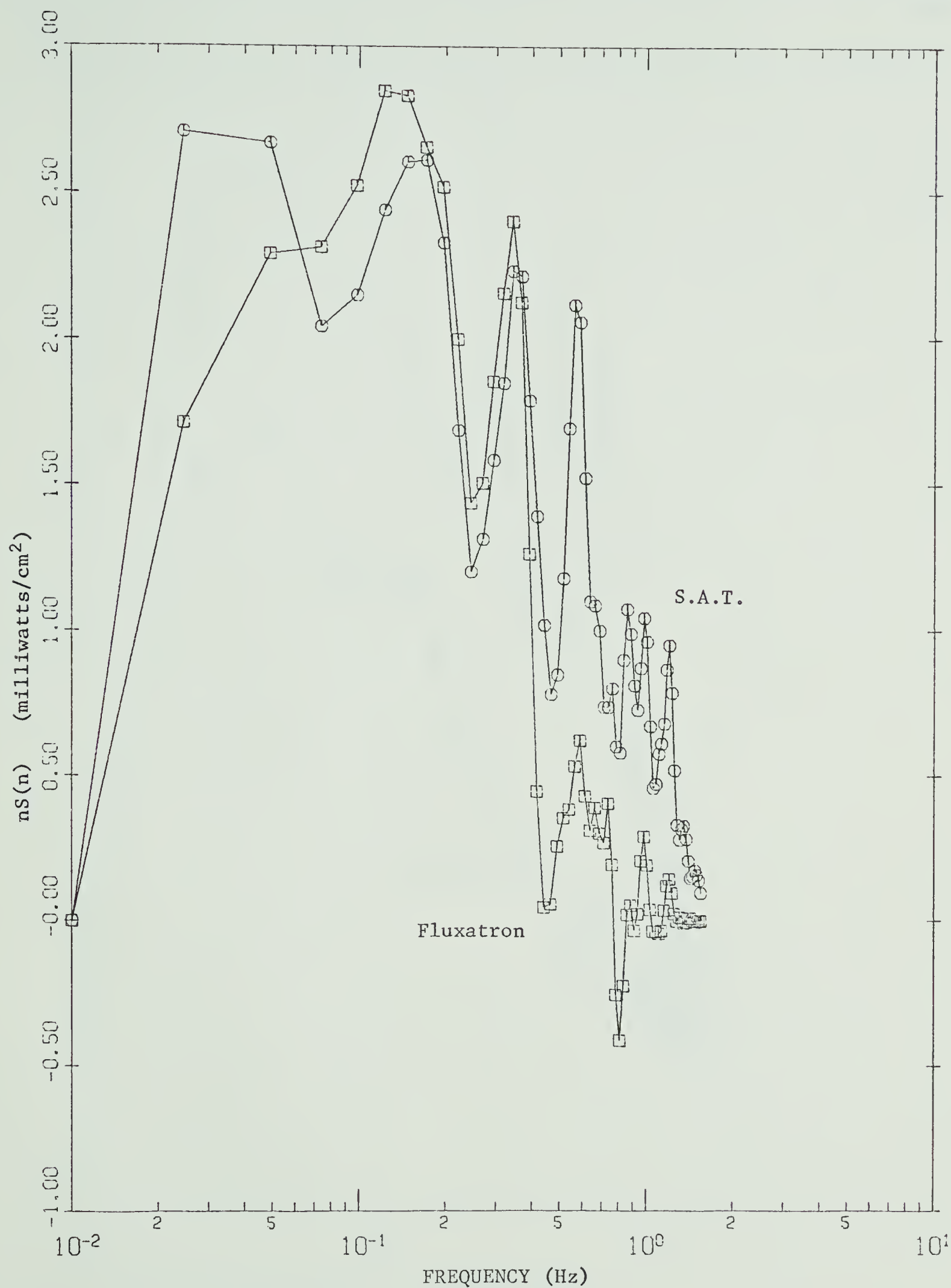


Figure 19 Absolute cospectra between wind and temperature over the low frequency range of analysis.

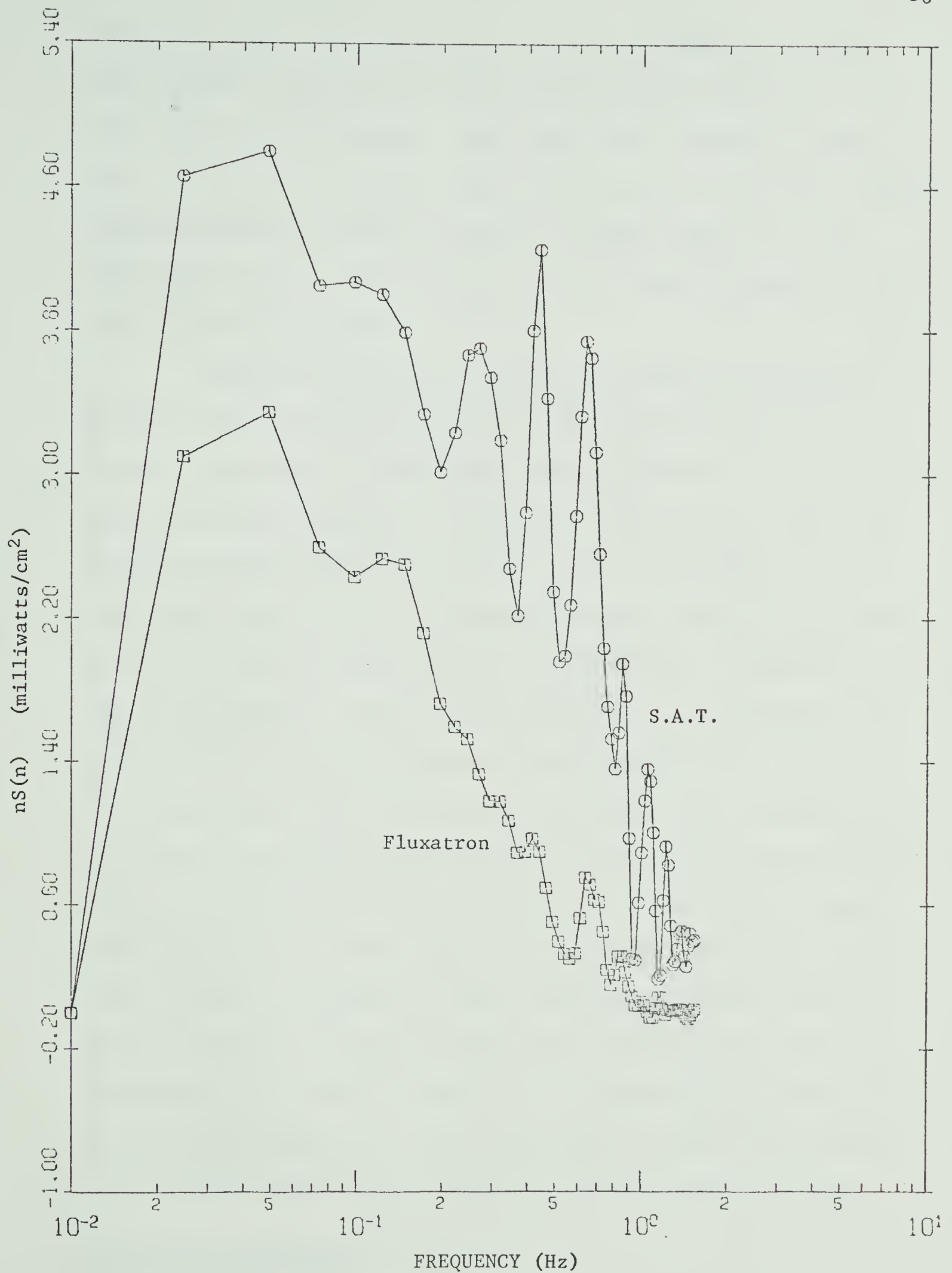


Figure 20 Absolute cospectra between wind and temperature over the low frequency range of analysis.

McBean and Miyake (1971) reported a cospectral maximum of $f = 0.1$ under unstable conditions with this peak shifting as high as $f = 1.0$ under stable stratifications. Pond et al (1971) reported a cospectral peak at $f = 0.2$ for analysis of data collected over the ocean. Earlier, Panofsky and Mares (1968) had reported the peak value at $f = 0.1$, again with a definite shift of the cospectra toward increasing frequency with increasing stability.

Figures 21 and 22 are plots of the normalized cospectra between wind and temperature, based on the same data as Figures 17 and 18, respectively. As with the absolute cospectra, the square plot symbols represent analyses of the fluxatron data, and the round plot symbols represent analyses of the S.A.T. data. The solid, straight lines have a slope of $-5/3$. The cospectra were normalized by dividing by the covariance between the wind and temperature as computed from the digitized data. Both plots show quite close agreement with the $-5/3$ law over the frequency range of approximately 0.1 to 1.0 Hz. For these samples this is the maximum range over which agreement could be expected because the cospectral peak, and hence the energy-production region, is slightly less than 0.1 Hz and the filter cutoff becomes effective at about 1.0 Hz. Kukharets and Tsvang (1969) have reported that the heat flux spectra at large wave numbers decrease much more steeply than $-5/3$, and they suggest that a slope of -2.6 is more representative of observed conditions. No evidence of a steeper slope has been found during the present experiment, with the data appearing to fit a $-5/3$ slope quite well over the analyzed frequency range.

Comparative Heat Fluxes

The final stage of analysis was to compute comparative heat

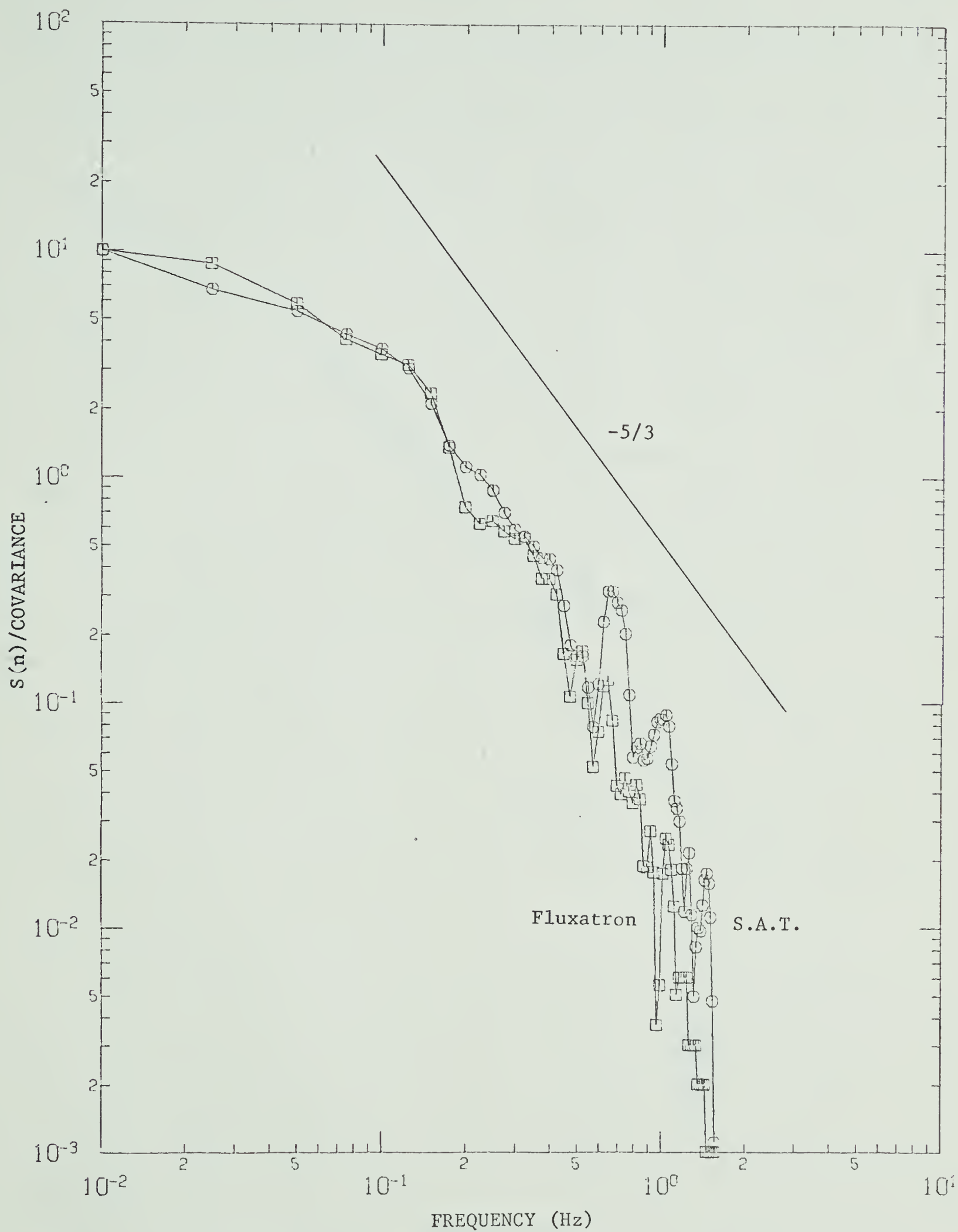


Figure 21 Normalized cospectra between wind and temperature over the low frequency range of analysis.

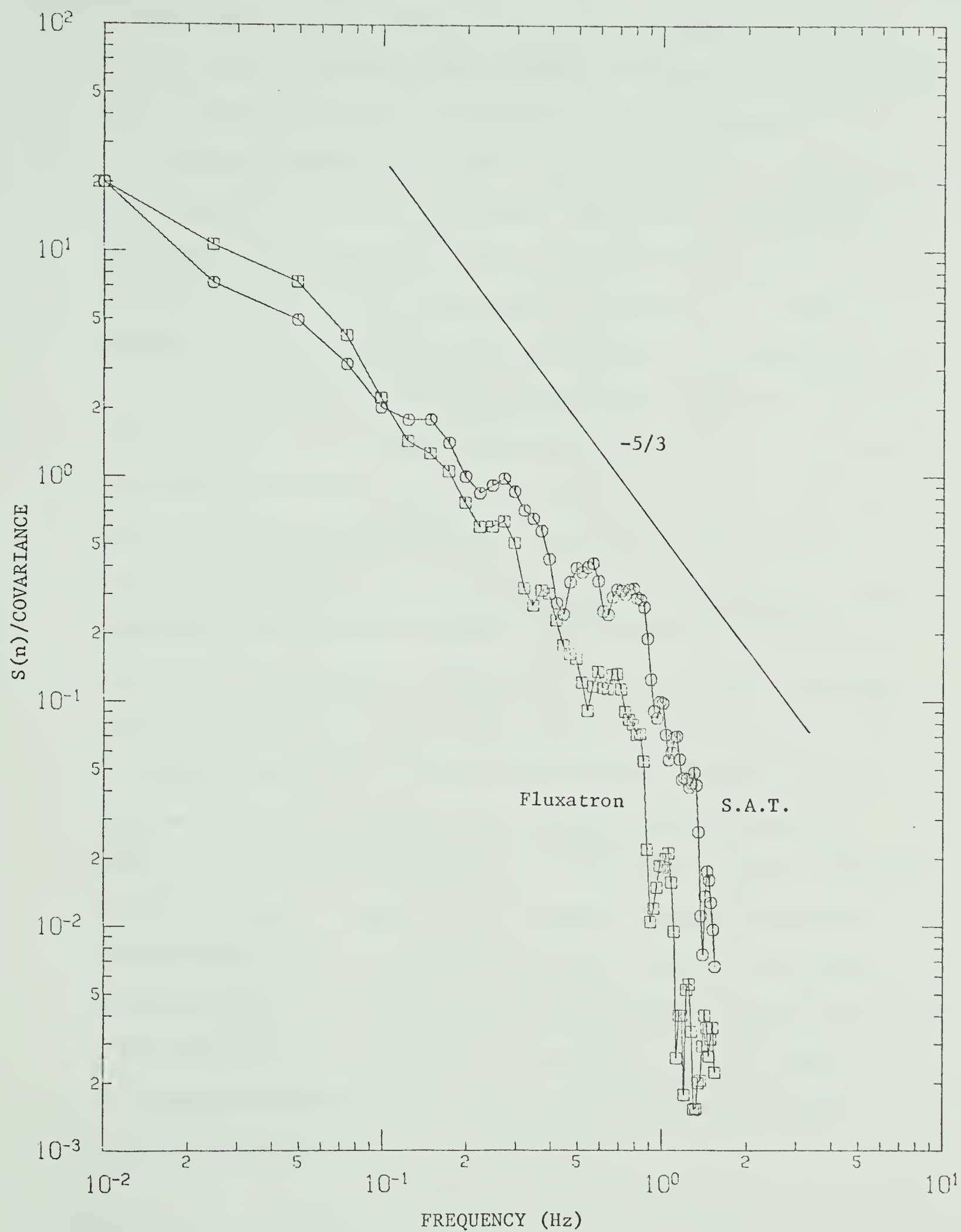


Figure 22 Normalized cospectra between wind and temperatures over the low frequency range of analysis.

fluxes. This has been done by integrating the cospectrum over frequency, and for comparison, by computing covariances from the digitized data. Tables 5 and 6 show the results of these calculations. The calculations were done on ten data samples of length ten minutes each, for both the S.A.T. and the fluxatron. The fluxes, as measured by the S.A.T. were consistently higher than those of the fluxatron. The average ratio was 1.9 when calculated by integrating the cospectra, and was 2.0 when calculated from the covariances of the digitized data.

From Table 4 it is noted that the measurements of temperature fluctuations by the two instruments agree very well, and Table 3 shows the wind fluctuations as measured by the S.A.T. as about 30 per cent higher than those of the fluxatron. The factor of two between the two heat flux measurements is interpreted as being caused by the poor response of the propeller anemometer to low amplitude fluctuations, with this effect apparently being more noticeable at low frequencies. Since the cospectral peak was found at 0.09 Hz and the variance peak of vertical wind was at 0.3 Hz, the non-linearity of the propeller response had a more noticeable effect on the heat flux cospectra than on the spectra of vertical wind. This point is further illustrated in Figure 5 which is a plot of low frequency coherence between the two wind measurements. The coherence had its maximum values between 0.1 Hz and 1.0 Hz, and dropped off at high frequency because of the limited high frequency response of the propeller, and decreased at low frequencies because of the non-linearity of response to low amplitude fluctuations.

TABLE 5

<u>HEAT FLUXES FROM INTEGRATION OF COSPECTRA</u>				
RUN NO.	SAMPLE NO.	S.A.T. FLUX (mw/cm ²)	FLUXATRON FLUX (mw/cm ²)	RATIO S.A.T./FLUXATRON
1	1	16.3	8.9	1.8
1	2	20.2	7.4	2.7
2	1	19.4	6.9	2.8
2	2	22.9	14.1	1.6
3	1	22.7	6.5	3.5
3	2	24.5	12.2	2.0
4	1	18.1	16.6	1.1
4	2	14.9	15.3	1.0
5	1	12.9	11.0	1.2
6	1	9.2	7.4	<u>1.2</u>
MEAN				1.9

TABLE 6

<u>HEAT FLUXES FROM COVARIANCES OF DIGITIZED DATA</u>				
RUN NO.	SAMPLE NO.	S.A.T. FLUX (mw/cm ²)	FLUXATRON FLUX (mw/cm ²)	RATIO S.A.T./FLUXATRON
1	1	19.3	10.9	1.8
1	2	24.8	7.9	3.1
2	1	22.4	8.0	2.8
2	2	25.4	15.2	1.7
3	1	29.1	6.9	4.2
3	2	28.9	13.6	2.1
4	1	19.8	19.0	1.0
4	2	16.6	18.0	0.9
5	1	15.1	12.1	1.2
6	1	10.9	8.4	<u>1.3</u>
MEAN				2.0

CHAPTER VI

SUMMARY

The objective was to measure comparative heat fluxes using two completely independent instruments, and from these comparisons, to make a relative assessment of the two instrument systems. The S.A.T. and the fluxatron were constructed at the University of Alberta and this experiment also served as an initial instrument test.

Throughout the first tests, numerous problems were encountered with instrument calibrations. Most of these were solved, but some were not. The temperature data from the fluxatron are unreliable because of uncertain calibrations. This problem can be easily solved during the next field season. The high frequency limitation of the propeller anemometer is a function of the known sensor response time. The non-linearity of the propeller response at low wind speeds is a more serious problem in this type of experiment and would be difficult to correct.

With proper calibrations the two instruments measure temperature fluctuations quite reliably over a large enough frequency range to be useful for flux measurements. The S.A.T. appears to measure fluctuations of vertical wind accurately, although further tests should be made. The fluxatron's propeller anemometer is not as reliable an instrument for measuring vertical wind fluctuations, particularly under conditions of light vertical winds. From this assessment of the two instruments it appears that the S.A.T. is the

more reliable of the two for measuring heat fluxes.

For further comparative experiments of this type, besides solving the various calibration problems, it is recommended that the time period of the samples be greatly increased, so as to minimize large sample fluctuations. However, the sample length can not be increased to the point where non-stationarity of the time series becomes a problem. Arriving at such an optimum sample length is particularly important for heat flux calculations, where smaller samples exhibit very large sample fluctuations.

BIBLIOGRAPHY

- Barret, E., and V. E. Suomi, 1949: Preliminary report on temperature measurements by sonic means, J. Meteor., 6, 273-276.
- Bingham, C., M. D. Godfrey, and J. W. Tukey, 1967: Modern techniques of power spectrum estimation, I.E.E.E. Transactions on Audio and Electroacoustics, AU-15, 56-66.
- Blackman, R. B., and J. W. Tukey, 1958: The Measurement of Power Spectra, Dover Publications, Inc., New York, 190 pp.
- Busch, N. E., and H. A. Panofsky, 1968: Recent spectra of atmospheric turbulence, Quart. J. Roy. Meteor. Soc., 94, 132-148.
- Businger, J. A., and M. Miyake, 1968: Justification for neglecting the third moment in the steady state expression for the turbulent heat-flux near the ground, Quart. J. Roy. Meteor. Soc., 94, 206-207.
- Businger, J. A., M. Miyake, A. J. Dyer, and E. F. Bradley, 1967: On the direct determination of the turbulent heat flux near the ground, J. Appl. Meteor., 6, 1025-1032.
- Businger, J. A., M. Miyake, E. Inoue, Y. Mitsuta, and T. Hanafusa, 1969: Sonic anemometer comparison and measurements in the atmospheric surface layer, J. Meteor. Soc. Japan, 47, 1-11.
- Cochran, W. T., et al, 1967: What is the fast Fourier transform? I.E.E.E. Transactions on Audio and Electroacoustics, AU-15, 45-55.
- Davidson, B., and H. Lettau, 1953: The great plains turbulence program, Weatherwise, 6, 166-169.
- Dyer, A. J., 1961: Measurements of evaporation and heat transfer in the lower atmosphere by an automatic eddy-correlation technique, Quart. J. Roy. Meteor. Soc., 87, 401-412.
- Dyer, A. J., B. B. Hicks, and K. M. King, 1967: The fluxatron - a revised approach to the measurement of eddy fluxes in the lower atmosphere, J. Appl. Meteor., 6, 408-413.
- Dyer, A. J., and F. J. Maher, 1965: Automatic eddy-flux measurement with the evapotron, J. Appl. Meteor., 4, 622-625.
- Gurvich, A. S., 1959: Acoustic microanemometer for investigation of the microstructure of turbulence, Acoustic J. (USSR), 5, 368-369.

- Hicks, B. B., 1970: The measurement of atmospheric fluxes near the surface: a generalized approach, J. Appl. Meteor., 9, 386-388.
- Jenkins, G. M., 1961: General considerations in the analysis of spectra, Technometrics, 3, 133-166.
- Kaimal, J. C., and J. A. Businger, 1963: A continuous wave sonic anemometer-thermometer, J. Appl. Meteor., 2, 156-164.
- Kaimal, J. C., and J. A. Businger, 1963: Preliminary results obtained with a sonic anemometer-thermometer, J. Appl. Meteor., 2, 180-186.
- Kukharets, V. P., and L. R. Tsvang, 1969: Spectra of the turbulent heat flux in the atmospheric boundary layer, IZV., Atmospheric and Oceanic Physics, 5, 1132-1142.
- Lumley, J. L., and H. A. Panofsky, 1954: The Structure of Atmospheric Turbulence, John Wiley & Sons, Inc., New York, 239 pp.
- MacCready, P. B., 1953: Structure of atmospheric turbulence, J. Meteor., 10, 434-449.
- McBean, G. A., 1971: The variations of the statistics of wind, temperature and humidity fluctuations with stability, Boundary Layer Meteorology, 1, 70-89.
- McBean, G. A., and M. Miyake, 1971: Turbulent transfer mechanisms in the atmospheric surface layer, unpublished manuscript, Institute of Oceanography, University of British Columbia.
- Mitsuta, Y., 1966: Sonic anemometer-thermometer for general use, J. Meteor. Soc. Japan, 44, 12-24.
- Miyake, M., et al, 1970: Comparison of turbulent fluxes over water determined by profile and eddy correlation techniques, Quart. J. Roy. Meteor. Soc., 96, 132-137.
- Miyake, M., R. W. Stewart, and R. W. Burling, 1970: Spectra and cospectra of turbulence over water, Quart. J. Roy. Meteor. Soc., 96, 138-143.
- Panofsky, H. A., and E. Mares, 1968: Recent measurements of cospectra for heat flux and stress, Quart. J. Roy. Meteor. Soc., 94, 581-585.
- Pond, S., et al, 1971: Measurements of the turbulent fluxes of momentum, moisture and sensible heat over the ocean, unpublished manuscript, Institute of Oceanography, University of British Columbia.

- Pond, S., et al, 1966: Spectra of velocity and temperature fluctuations in the atmospheric boundary layer over the sea, J. Atmos. Sci., 23, 376-386.
- Pond, S., R. W. Stewart, and R. W. Burling, 1963: Turbulence spectra in the winds over waves, J. Atmos. Sci., 20, 319-324.
- Priestley, C. H. B., 1959: Turbulent Transfer in the Lower Atmosphere, The University of Chicago Press, 130 pp.
- Schotland, R. M., 1955: The measurement of wind velocity by sonic means, J. Meteor., 12, 386-390.
- Sitaraman, V., 1970: Spectra and cospectra of turbulence in the atmospheric surface layer, Quart. J. Roy. Meteor. Soc., 96, 744-749.
- Swinbank, W. C., 1951: The measurement of vertical transfer of heat and water vapour by eddies in the lower atmosphere, J. Meteor., 8, 135-145.
- Wesely, M. L., G. W. Thurtell, and C. B. Tanner, 1970: Eddy correlation measurements of sensible heat flux near the earth's surface, J. Appl. Meteor., 9, 45-50.
- Zubkovskiy, S. L., and B. M. Koprov, 1969: Experimental investigation of the spectra of turbulent heat and momentum fluxes in the atmospheric surface layer, IZV., Atmospheric and Oceanic Physics, 5, 323-331.

B29988